Organisation of Islamic Cooperation

Design and Result Analysis of Round Core Optical fibre PCF with High Sensitivity, Low EML and a low Confinement Loss.

Prepared by

Osamah Abdullah Yahya Amran

(ID- 160021145)

Muhammad Ahmad kafur

(ID- 160021171)

Supervised by

Dr. Md. Rezaul Hoque khan

Associate Professor

A Thesis Submitted to the Academic Faculty in Partial Fulfilment of the Requirements for the Degree of

Bachelor of Science in Electrical and Electronic Engineering

ACKNOWLEDGEMENT

First of all, we have no words to express our deepest gratitude to the Almighty Allah (SWT), who has enabled us to successfully complete our research thesis..

We would like to express our deepest and sincere appreciation for their affection, encouragement and inspiration throughout our lives. We hereby honor our parents uniquely. Thanks to both of you for giving us the power to reach for the stars. Much obliged to place your hopes on you and to trust in us. We would never have been the people we are today without you. With positivity and enthusiasm, thank you for helping us to shape our lives. We can say how happy and grateful we are to you with no words. We would like to thank you for everything. First of all, we have no words to express our deepest appreciation to the Almighty Allah (SWT), who has made it possible for us to successfully complete our research thesis. Second, we would like to express our special appreciation to the supervisor and instructor of our research, Dr. Md. Rezaul Hoque Khan, who gave us the golden opportunity to do this wonderful research on DESIGN AND RESULT ANALYSIS OF ROUND CORE OPTICAL FIBRE PCF WITH HIGH SENSITIVITY, LOW EML AND LOW CONFINEMENT LOSS, which provides invaluable guidance in this research. We were deeply motivated by his dynamism, vision, honesty and inspiration. He taught us the methods for carrying out the experiments and presenting the research work as simply as possible. Working and learning under his guidance was a great pleasure and honour. We are immensely grateful for what he gave us That has also helped us to do our research and we have come to know so many new things that we are very grateful to you, sir, that would not have been possible without you. Finally, our gratitude goes to all our families, friends and also individuals who have assisted us directly or indirectly to complete the research work.

Osamah Abdullah Yahya Amran

Muhammad Ahmad kafur

Department of Electrical and Electronic Engineering

Islamic University of Technology (IUT)

Gazipur, Bangladesh

March 2021

CERTIFICATE

This is to certify that the thesis paper entitled "Design and Result Analysis of Round Core Optical fibre PCF with High Sensitivity, Low EML and a low Confinement Loss" submitted by Osamah Abdullah Yahya Amran (ID- 160021145),Muhammad Ahmad kafur(ID- 160021171) has been carried out under my supervision. This thesis has been prepared in partial fulfilment of the requirement for Degree of Bachelor of Science in Electrical and Electronics Engineering.

Approved by:

.....

Dr. Md Rezaul Haque Khan

Supervisor
Associate Professor
Department of Electrical and Electronic Engineering,
Islamic University of Technology (IUT), Board bazar, Gazipur-1704.

ABSTRCT

From this paper claims that high sensitivity, low effective materials loss (EML)is presented with a round core photonic crystal fiber (HC-PCF) in the terahertz frequency range can detect chemical analytes. Zeonex round-core analysis solution uses the Zeonex based round core with an analyte inside and It is surrounded by a series of circular air holes bounded by a perfectly matching layer (PML). Numerical analysis of the proposed sensor's performance is done by using COMSOL software. Because a round core has both high sensitivity and low transmission loss, it is commonly used in sensor applications. Complementarily, simplicity in design also aids manufacturability and ease of application across numerous diverse sectors.

CONTENTS

LIST OF FIGURES

Chapter 1

Introduction

1.1 Introduction

A particular class of fiber PCF has air holes in the cladding and is composed of a single substance with empty spaces inside the air. Structural parameters vary. A particular class of fiber PCF has air holes in the cladding and is composed of a single substance with empty spaces inside the air. Structural parameters vary in order to calculate how far the electromagnetic wave spreads such as the effective index mode, confinement loss, chromatic dispersion, and field mode diameter (hole diameter, lattice pitch, etc.), this feature has similar advantages in many instances It has only recently come to light because of its properties that are fiber optic aspects that have not been implemented in traditional optical fibers. So the PCF has received a lot of attention. The PCF has received a lot of attention. They are also known as "finally single-mode fibers" and are divided into two types of fibers, also known as "special types of fibers." Light is guided by a total internal reflection, with multiple air holes, between a solid core and a cladding region. The second on the other hand uses a structurally perfect periodic structure called photonic band gap fiber which guides light in a low index core region. In our design we used three different materials such as water, benzene and ethanol. These three materials are used to plot several different properties such as sensitivity, effective material loss (EML), containment loss, and birefringence. Knowing the difference in structural parameters allows you to precisely determine the quantity of all circulation uniqueness. One of the main ways in which the structural parameters serve to contain light in the core is by influencing the properties of propagation Since the ability to contain light in round or solid cores is something that PCF possesses optical fiber communications, fiber lasers, optical processors, photonic crystal diodes, and extremely sensitive liquid sensors all provide a strong detection sensitivity. Chromatic dispersion and loss of containment around the core PCF are discussed in this paper. The thickness of the layer in our design has changed from its previous value. The absorption of the outgoing waves is changed in equations, while the sensitivity is changed by the variation in the core diameter.

1.2 Evolution of Photonic Crystal Fiber

1.2.1 Photonic Crystal Fiber in brief

The PCF is a single material optical fiber consisting of a silica-air microstructure. It contains microscopic air-holes in a silica background running down length of the fiber that form the silica-air microstructure as well as the lower refractive index cladding [1]. Air-holes can be arranged in the cladding in a periodic (hexagonal arrangement being the common) or an aperiodic fashion. The core may either be a solid (made of silica) or a hollow (made of air). The former core type PCF guides light based on the modified TIR mechanism likewise conventional fibers. The later guides light based on a new mechanism which is known as the photonic band gap (PBG) [2].

For PCFs, it is not necessary that the core must be made of a higher refractive index material than the cladding. Similarly, it is also not necessary that only the TIR mechanism confines light into the core of all optical fibers. Inclusions of tiny air-channels in the cladding of PCFs offer a wider design space, i.e., a great flexibility in tailoring its properties [3]. Modulating the silica-air structure parameters, it is possible to design application specific guiding properties. PCFs show a number of unusual and previously unimaginable properties including endlessly single mode operation super high and low nonlinearities [4], very high or low birefringence [5], ultra-flattened and ultra-low chromatic dispersion and many others. Hence, PCFs can easily outperform conventional fibers in many scientific and technological areas of applications for their superior and easy to tailor optical properties.

Photonic Crystal Fiber (PCF) is a new class of optical fiber based on the properties of photonic crystals. Because of its ability to confine light in hollow cores or with confinement characteristics not possible in conventional optical fiber [6]. PCFs or holey fibers or microstructure optical fibers have a microscopic array of air channels running down their length that make a low index cladding around the undoped silica core [7]. PCF is now finding applications in fiber optic communications, nonlinear devices and dispersion compensating fibers, high-power transmission, highly sensitive gas sensors and other areas. Several parameter can be controlled in PCF such as air-hole shape and diameter, refractive index of the glass, type of lattice and distance between hole to hole that is lattice pitch. Solid or air core single mode fibers can be achieved.

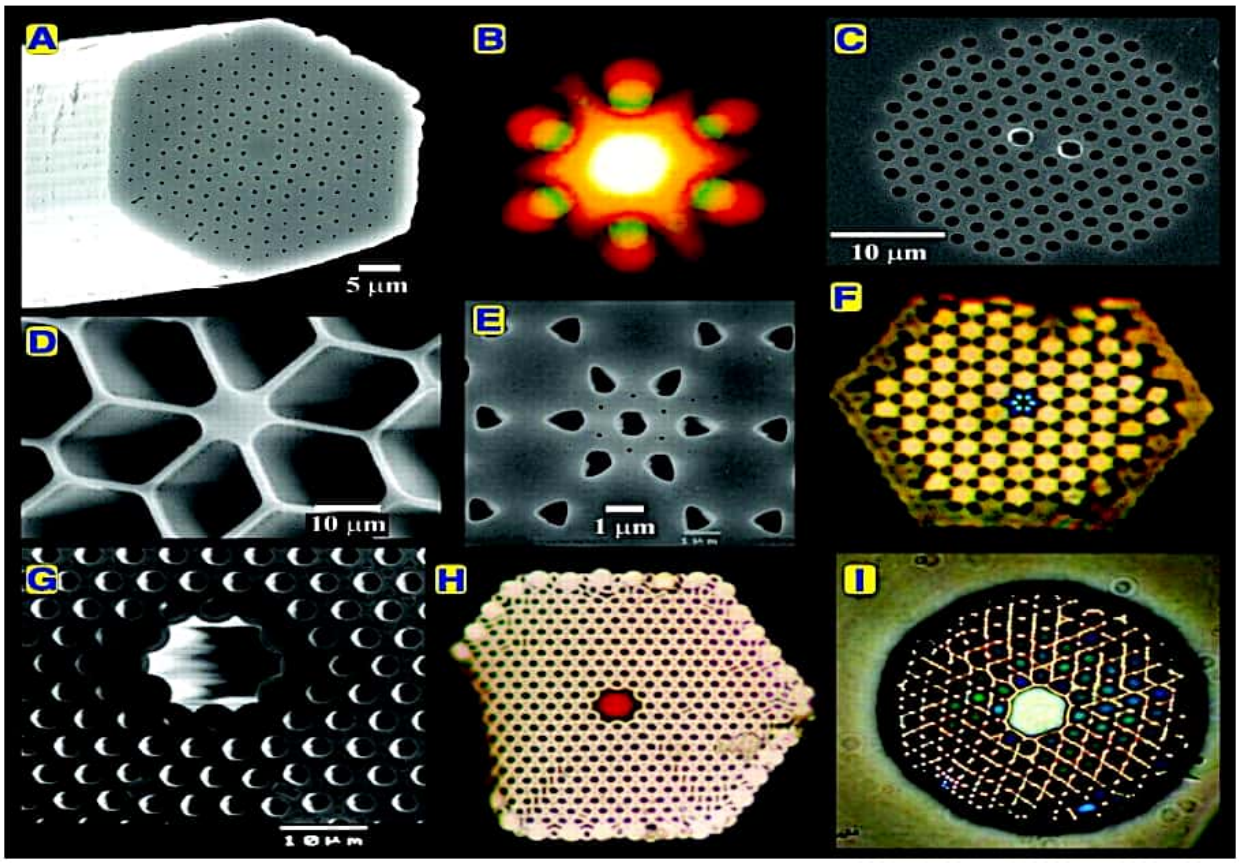

Fig.1.1 An assortment of optical (OM) and scanning electron (SEM) micrographs of PCF structures. (A) SEM of an endlessly single-mode solid core PCF. (B) Far-field optical pattern produced by (A) when excited by red and green laser light. (C) SEM of a recent birefringent PCF. (D) SEM of a small (800 nm) core PCF with ultrahigh nonlinearity and a zero chromatic dispersion at 560-nm wavelength. (E) SEM of the first photonic band gap PCF, its core formed by an additional air hole in a graphite lattice of air holes. (F) Near-field OM of the six-leaved blue mode that appears when (E) is excited by white light. (G) SEM of a hollow-core photonic band gap fiber. (H) Near-field OM of a red mode in hollow-core PCF (white light is launched into the core). (I) OM of a hollow-core PCF with a Kagomé cladding lattice, guiding white light.

1.2.2 History

In 1978, the idea of photonic crystal fiber was presented for the first time by Yeh *et al* [12]. They proposed to clad a fiber core with bragg grating, which is similar to 1D photonic crystal. A 2D photonic crystal fiber with an air-core was invented by P. Russell in 1992. And the first PCF was reported at the Optical Fiber Conference (OFC) in1996.

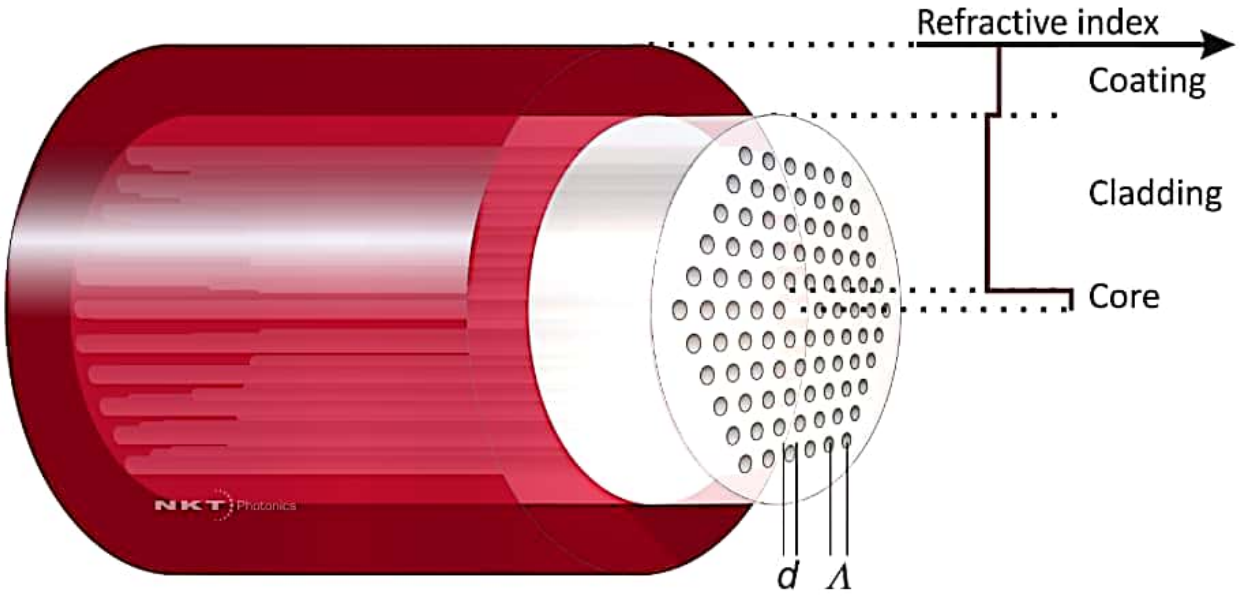

Fig.1.2 Overview of photonic crystal fiber development

In 2000, highly birefringent PCF was proposed at first [8]. Fabrication of bragg fiber was done in 2001for the first time. PCF laser with double cladding was also presented in 2001 [9]. In 2002, PCF with ultra-flattened dispersion was initiated which contents highly energy transmission in HC-PCF. Low loss transitions between different PCFs and photonic band-gap at 1% index contrast were pioneered in 2005. In the year 2008, polarization dependence of stimulated Brillouin scattering in small core PCFs was established for the first time. After that, non-linear inter-core coupling in triple core PCFs was launched in 2009 [9]. Then dispersion and non-linear coefficient of PCF were based on degenerate four wave mixing in 2010. In 2011, an oval kind of honeycomb porous-core PC-PBGF was firstly proposed.

1.3 Evolution of Hollow core PCF

1.3.1 HC-PCF in brief

Hollow core photonic crystal fibers (PCF) are one of the most interesting types of fibers with unique properties of light guidance in the air. A photonic band gap effect in the periodic structure of the photonic cladding allows light guidance in the low index core [6,7]. Hollow core PCFs allow a reduction of all phenomena related to the interaction between glass and light, since most of energy propagates in the air. Therefore dispersion, multiphoton absorption, Raman scattering and other nonlinear effects are dramatically reduced. A silica based hollow core PCF achieves a very low attenuation of 1.2 dB/km for 1.62 μm [8]. In this case 99.5% of energy in the fundamental mode propagates in the air. Further reduction of the attenuation to gain the

attenuation level of standard telecommunication optical fibers at 0.1 dB/m is uncertain because surface modes are created at the glass-air border near the core. Since their propagation constants can be very similar to the fundamental guiding mode, the modes can be coupled and energy is transferred from the fundamental to the surface modes [9]. Hollow core PCFs made of soft glasses witness higher attenuation since the attenuation of glass itself is much higher. However, due to their higher refractive index they are attractive components from which to build a new type of devices infiltrated with polymer or liquids e.g. liquid crystals [10].

1.3.2 History

Photonic crystal fibers (PCF) optical fibers whose cladding is microstructured—were first reported in late 90s and are fabricated using an original process called "stack-and-draw" technique. The versatility of this process and its ability to tailor the cladding modal spectrum by judiciously designing the cladding structure offered a platform to develop optical fibers with various core and claddings designs, and enabled novel optical guidance mechanisms and fibers with unprecedented linear and nonlinear properties. In turn, PCF has proved to be an excellent photonic component for multiple applications in varied fields such as supercontinuum generation in nonlinear optics, gas-based optics, and nonlinear optics.

Figure (2) illustrates, in a tree diagram, the PCF family and its diversity from the standpoint of the fiber structural designs, constitutive materials or the physics underlying their guidance mechanisms. If we had to classify these fibers by their structural architecture, we can identify two main families—solid-core and hollow-core fibers—each of them can be divided in several ways. For example, they can be classified by one of the three guidance mechanisms, which are (i) Modified Step Index (MSI), (ii) Photonic Bandgap (PBG), and (iii) Inhibited Coupling (IC). The fibers can also be categorized via their cladding geometry. The latter outstands with the impressive variety that can be found in each guidance mechanism, and the optical properties that can address. Among these, we can highlight the endlessly single-mode (ESM) fiber, which enables optical guidance in a single mode fashion regardless of the wavelength. This in turn led to the large mode area (LMA) single mode fibers, and subsequently to high-power fiber lasers. The PCF tree diagram also shows other designs that were developed such as enhanced birefringence (Hi-Bi) fibers, dispersion compensation PCF (Disp-Comp), all-solid PBG-guiding PCF, solid-core IC-guiding PCF, and hybrid guidance PCF to mention a few. Finally, we can record PCF via their constitutive materials. Here, whilst silica remains the dominant material used, a lot of effort is currently undertaken to use alternative materials such as soft glass or chalcogenides mainly driven by either further enhancing optical nonlinearities in PCF or extending their transmission well beyond the silica transparency window [11].

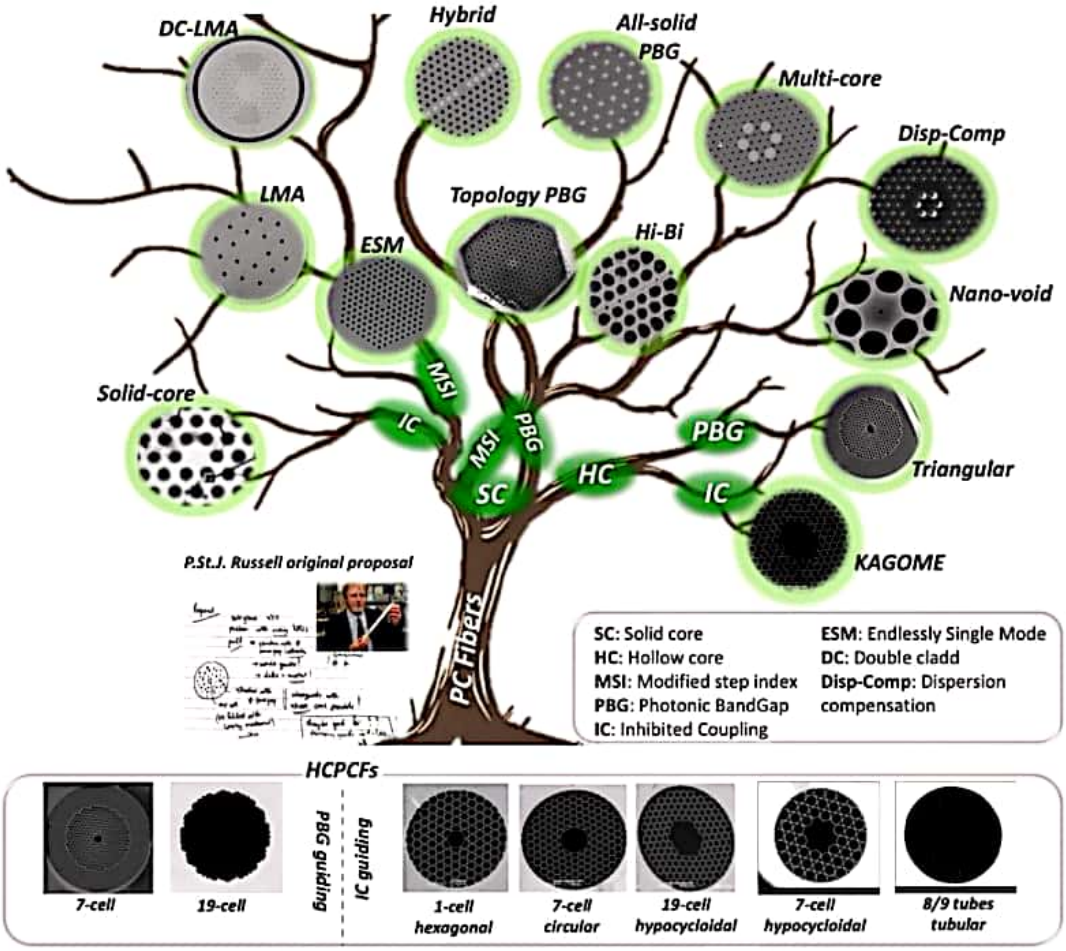

Fig.1.3 Photonic crystal fibers family tree diagram (top). Micrographs of HCPCF-based on PBG guidance and IC guidance.

1.4 Motivation

Optical signals are transmitted over the optical links. Different wavelength components of signal will generally experience different propagation time because transport medium has different refractive indices for different wavelengths. In the recent period, the demand for transmission capacity and bandwidth are becoming more and more challenging [12]. Under this situation, optical fiber is the most favorable delivering media in information industry, with its huge bandwidth and excellent transmission performance. The main goal of any communication system is to increase the transmission distance. Loss and dispersion are the major factors that affect fiber optic communication. The dispersion causes broadening of optical pulses when transmitted through the fiber. Thus, the dispersion must be compensated in the long distance optical data transmission system to nullify the effect of pulse broadening. Dispersion

compensating fibers (DCF) are widely used for dispersion compensation which is designed to have large negative dispersion [13]. It is difficult to achieve high negative dispersion using the conventional DCF.

Now-a-days PCF has become a promising candidate especially as a dispersion compensator. It allows to tune dispersion properties in a way which is not possible for the conventional fibers [17]. In conventional fibers, the chromatic dispersion is controlled by using air-holes with same diameter in cladding region. Using this design technique, it is difficult to control the dispersion slope in wide wavelength range [14]. PCF has great controllability in dispersion by varying the hole diameter and hole to hole spacing. Moreover, PCF offers design flexibility and show the property of bi-refringence, low confinement loss and nonlinearity [15].

Prism coupled-based biosensors are broadly employed because of the ease of usages. However, it is bulky and includes moving optical and mechanical parts, which limit its application in remote sensing [16]. On the contrary, HC provide greater sensitivity. As a result, a small variation of an analyte's RI can be detected from the large peak wavelength shift.

1.5 Major objectives

The main aim is to design a simple high sensitive with the following specific objectives :

1. To use hollow core for better sensing and transforming
2. To introduce newer structure
3. To change the RI of analyte
4. To change the air hole diameter and pitch.
5. To determine the linearity of the sensor and figure of merit

1.6 Application

PCF is used in many significant purposes in optical fiber communication it plays a great role. The applications of PCF are described below-

1.7 Dispersion managed applications

Although PCFs offer great design flexibility, design of nearly-zero dispersion-flat PCF (NZDF-PCF) which is required in almost all applications is remaining a big challenge for the designers, This is due to the fact that for most dispersion managed applications, a low confinement loss is also required in addition to dispersion-flat characteristics [17]. Therefore, designers use either PCFs with many rings of air-holes [18] to reduce the confinement losses or PCFs with non-uniform cladding [19] to achieve simultaneously dispersion-flat curve and low confinement

losses. The former design technique is not only unsuitable for wideband dispersion management [20] but also results in an increased holey cladding region and increased fabrication challenges [21]. Reportedly the later technique, although being frequently used, also sets a great fabrication difficulty because of non-uniform cladding. A non-uniform cladding i.e., air-hole modulation results in increased design parameters that further affects fabrication and tolerance. These challenges exist to date and need to overcome by adopting novel design techniques

1.7.1 Nonlinear optics applications

Nonlinear PCFs (HNL-PCFs) are suitable for nonlinear-optics applications namely optical parametric amplification, super continuum generation, soliton generation, and wavelength converters [22]. The major challenge associated with designing highly nonlinear PCFs is setting the zero dispersion wavelength around the telecom window because a PCF with a short pitch and uniform smaller air-hole dimensions tends to shift the zero-dispersion wavelength towards shorter wavelengths [23] and a PCF with higher air-hole dimension relative to the pitch sets a limit on the single mode operation bandwidth [24]. Therefore, it is crucial to optimize the air-hole dimension and pitch restoring design simplicity at the same time. Moreover, confinement loss control and sensitivity to parameter variations become major issues as HNL-PCFs use a smaller pitch value. A smaller pitch results in a higher confinement loss and higher sensitivity to parameter variations [25]. The same challenge exists to date which needs to be addressed efficiently. But it is not used in my thesis because I find out low nonlinearity.

1.7.2 Telecommunication applications

At the beginning of PCF technology, it was being considered for only optical device applications and not as a data transmission media. This was due to high optical losses of such fibers [26]. Recently, utilizing sophisticated and accurate design and fabrication techniques, the optical losses have been reduced to a 0.28 dB/km [27]. Therefore, interest is growing to rethink PCFs as a transmission media for future reconfigurable data transmission applications [28]. PCFs with large mode area are suitable for such applications. Although, there are reports addressing this issue, there are some other issues related to large mode area PCFs (LMA-PCFs) design.

1.7.3 Sensing Applications

Highly birefringent PCFs (HB-PCFs) are suitable for sensor applications. Designing highly birefringent PCFs require breaking the symmetry between the fiber axes or applying stresses in the cladding [29]. Such changes in PCF claddings impose fabrication difficulties as well as other difficulties associated with designing nearly-zero dispersion and low confinement losses. It is due to the fact that birefringent fibers are supposed to have near-zero dispersion at the

target wavelength to suit practical applications [30]. This is also an ongoing challenge and needs a special design care to overcome.

1.8 Major Contribution

The overall objective of the book is to focus ways to design and enhance the sensitivity of PCF based sensor. The main objective of this work is to design and characterize PCFs for high birefringence and to make the resonant peak sharper for the based sensor applications.

Our thesis work has the following results:

The proposed round shape sensor shows maximum wavelength interrogation sensitivity of 8000 nm/RIU with resolution of 1.25×10^{-5} RIU. Moreover maximum amplitude sensitivity 560 RIU^{-1} with resolution of 1.78×10^{-5} RIU is obtained in the sensing range from 1.45-1.48.

1.9 Chapter Organization

And future work We organize our whole thesis book into 3 chapters. A brief overview of the chapters are as follows-

Chapter 1 covers general introduction of the thesis.

Chapter 2 covers basic properties of photonic crystal fiber and Round core photonic crystal fiber.

Chapter 3 deals with simulation and methodology of the thesis.

Chapter 4 includes Conclusion

Chapter 2

Basic Properties of Photonic Crystal Fiber and Surface Plasmon Resonance

2.1 Overview

In this chapter, we discuss basics of photonic Crystal Fiber (PCF), different types of PCF, PCF versus conventional optical fiber, Light guiding mechanism of PCF with total internal reflection and photonic band gap. We also discuss the properties of PCF and SPR. Properties of PCF includes refractive index, chromatic dispersion, bi-refringence, confinement loss, effective area and dispersion slope. , evanescent field, wavelength sensitivity, amplitude sensitivity and figure of merit (FOM).

2.2 Conventional Photonic Crystal Fiber

Photonic crystal fibers (PCFs) consisting of a periodic distribution of air holes along its length and a defect region in its center, have been intensively studied in recent years due to their unique optical properties [31]. In conventional PCFs, the core-guidance of the optical signal is provided by a solid silica defect core surrounded by periodic air-hole array in the cladding. Since the core refractive index is higher than the effective cladding index, which is an average of air holes and background silica, light signal can be guided by the total internal reflection along the silica defect core similar to conventional optical fibers. The PCF is a single material optical fiber consisting of a microscopic array of air channels running down the entire fiber length. These air-holes in a silica base constitute the low index cladding and the core is generally formed either by removing a central air-hole from the structure or by creating a larger air-hole in its position. The former one with a missing hole, i.e., with a solid core is called a high index core (HIC)/ index-guiding (IG) PCF and the later with an air-core is called a hollow core (HC)/ low index core (LIC)/ PBG PCF .Fig. 2.1 shows cross sectional views of both the high index and low index core PCFs. In the figure air holes are represented by small unfilled circles. The absence of an air hole is denoted by a dotted small circle .Inclusions of air-holes in the PCF offer a variable index-contrast between the core and the cladding which is achieved by changing dimensions of holes and cladding geometry. Thus, PCFs have a number of design freedom namely, air-hole diameter, air-hole to air hole distance (the pitch), core radius, and number of rings. Since the guiding properties of optical fibers depend on the refractive index and the refractive index of PCFs depends on those design freedoms, application specific guiding properties can be achieved by modulating those parameters [32].

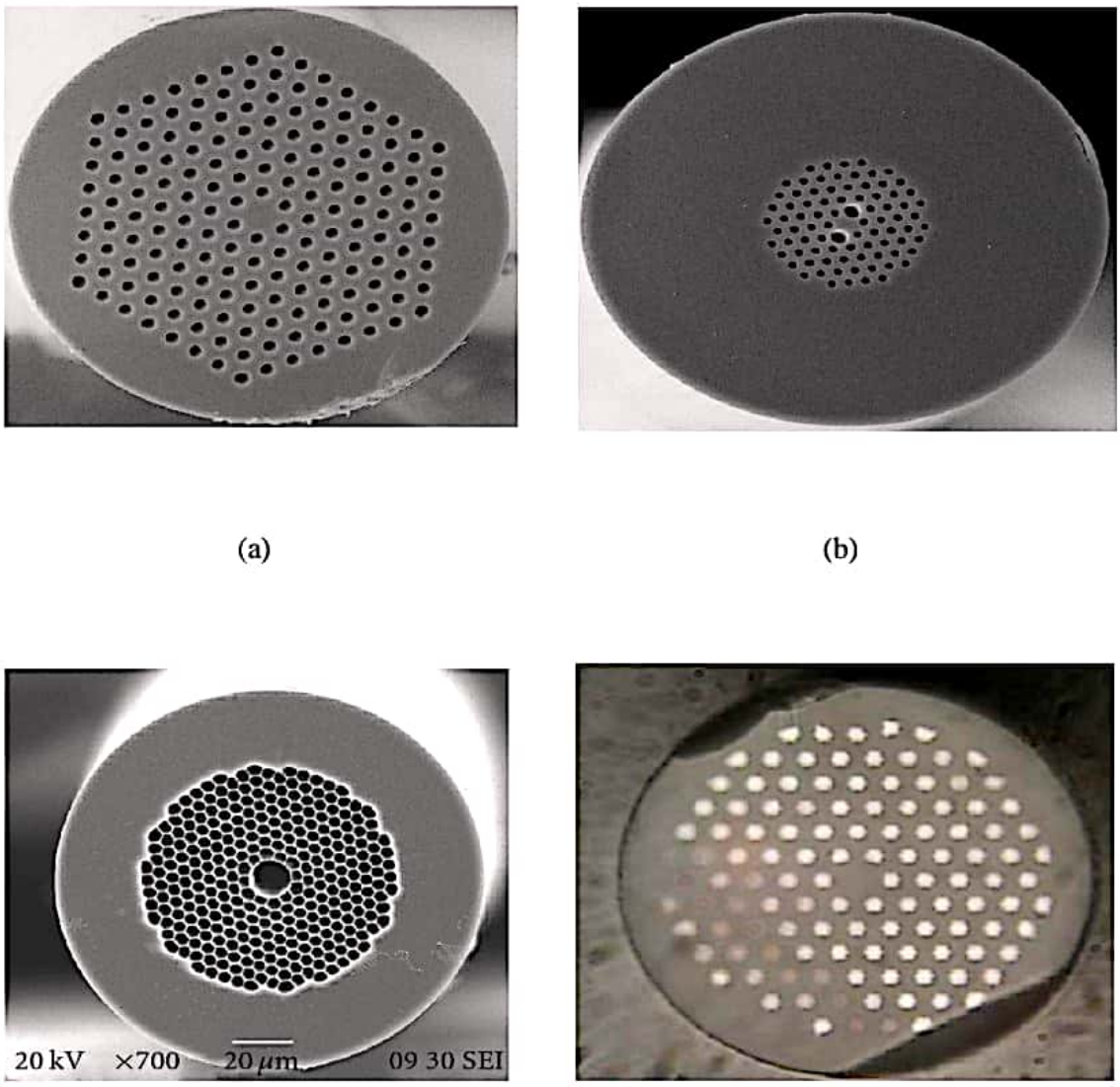

Fig.2.1 Scanning electron micrographs of different PCF cross-sections. (a) a large-mode-area air-silica endlessly single-mode PCF, (b) an air-silica highly birefringent PCF, (c) an air-silica air-core PBF. These PCFs are from Crystal Fiber A/S (d) an all-solid PBF

2.3 Different Classes of PCF

PCFs can further be classified into a number of other types [33] depending on the dimensions of the fiber parameters, structures, and specific guiding properties. IG-PCFs are classified as HNL fibers (having very small core dimensions to provide tight mode confinement), LMA fibers (having larger dimension of the core and small refractive index contrasts to allow spreading out of the guiding light to provide a larger effective area), and high numerical aperture (HNA) fibers (having a microstructure cladding surrounded by a ring of air-holes with larger dimensions). Moreover, IG-PCFs that have a doped core (high index material doped silica) and a holey cladding are called hole assisted PCFs (HA-PCFs). PBG-PCFs are classified as air-guiding (AG)/ HC fibers, LIC fibers, or Bragg fibers. Fig.2.1 shows examples of all these microstructure fibers types. PCFs can again be of another type namely polarization maintaining (PM) fibers having either a stress applying part or an asymmetric cladding structure to maintain a linear state of polarization. Again, likewise conventional fibers, PCFs are also classified as single mode or multi-mode fibers depending on the number of modes supported by a particular PCF (IG or PBG).

(a)

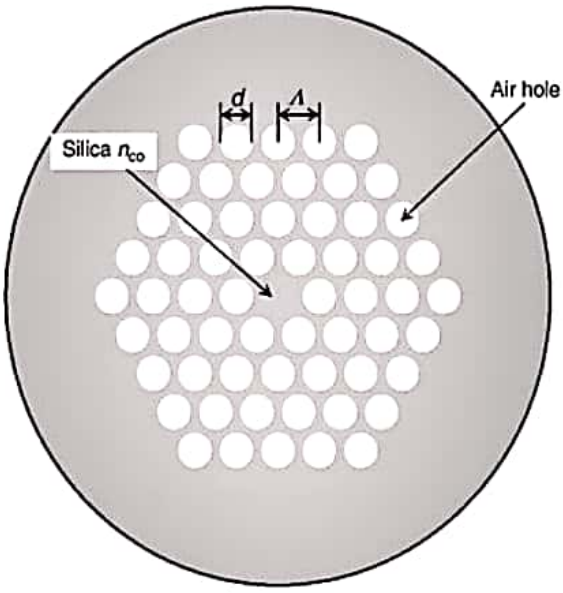

(b)

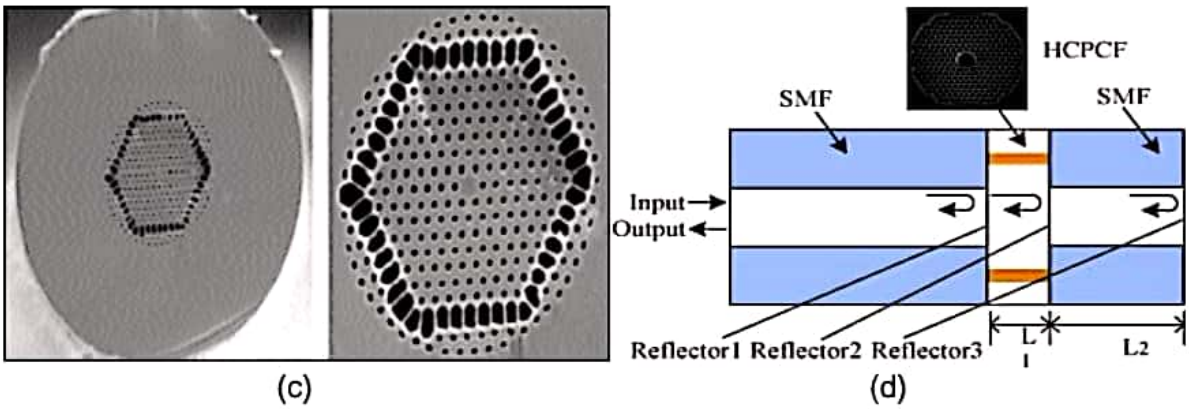

Fig.2.2Types of PCFs (a) PM-PCF, (b) HA-PCF, (c) HNA-PCF, and (d) Bragg Fiber- a special type of HC-PCF [30].

2.4 PCF versus Conventional Optical Fiber

An ordinary optical fiber is made of a core which has a higher refractive index than that of the cladding. The refractive index of the core is made higher than that of the silica cladding by doping a high refractive index material in the core region. A commonly used material is the germanium for increasing the refractive index and a commonly used material for decreasing the refractive index is the Fluorine.

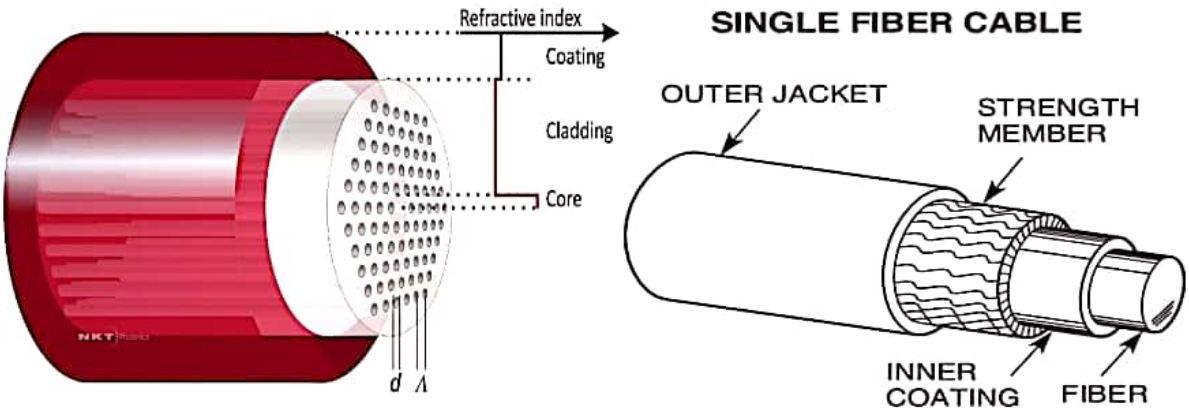

Fig.2.3 Schematic cross sections and index-profiles of (a) PCFs (a missing air-hole in the center represents the core) and (b) Ordinary fibers .

On the other hand the PCF is, as stated earlier, a single material fiber that contains tiny air-holes in a silica background. The two types of fibers are illustrated in the Fig.2.2. Index contrast between the core and the cladding of conventional fibers is very low but it is high and manageable for PCFs simply by tuning difference between the two fibers which makes significant differences in their optical properties [34]. The later shows super high or low nonlinearities, high birefringence, flat dispersion, wider single mode operation, and many others [35].

2.5 Light Guiding Mechanism of PCF

PCFs guide light based on two mechanisms, namely, the TIR mechanism and the PBG mechanism [35]. If the PCF guides light based on the TIR mechanism, it is called an IGPCF or a HIC-PCF. On the other hand if the light guiding is based on the PBG mechanism, it is called a PBG-PCF, or LIC-PCF, or HC-PCF.

It has been illustrated in Fig. 2.3(a) that IG-PCFs generally omit a single air-hole from the structure. This type of PCFs can also have a high index material (e.g. Ge) doped core. In either case, the core must have a high refractive index ($n_{core} > n_{cladding}$) than that (equivalent refractive index) of the cladding. Unlike IG-PCFs, PBG PCFs have a hollow core ($n_{core} > n_{cladding}$) which is generally created by placing a larger air-hole in the center as shown in Fig 2.3(b)

2.5.1 Total Internal Reflection of PCF

The basic principle for the guiding light in conventional fibers is well known as total internal reflection (TIR). The most typical TIR crystal fibers have solid core surrounded by a cladding with a regular periodic array of air holes. These air holes make the effective refractive index of cladding region lower than pure silica, so light confines to the solid core area, which has a relatively higher refractive index [8]. A schematic cross section of such PCF is given bellow which shows the propagation of light with TIR.

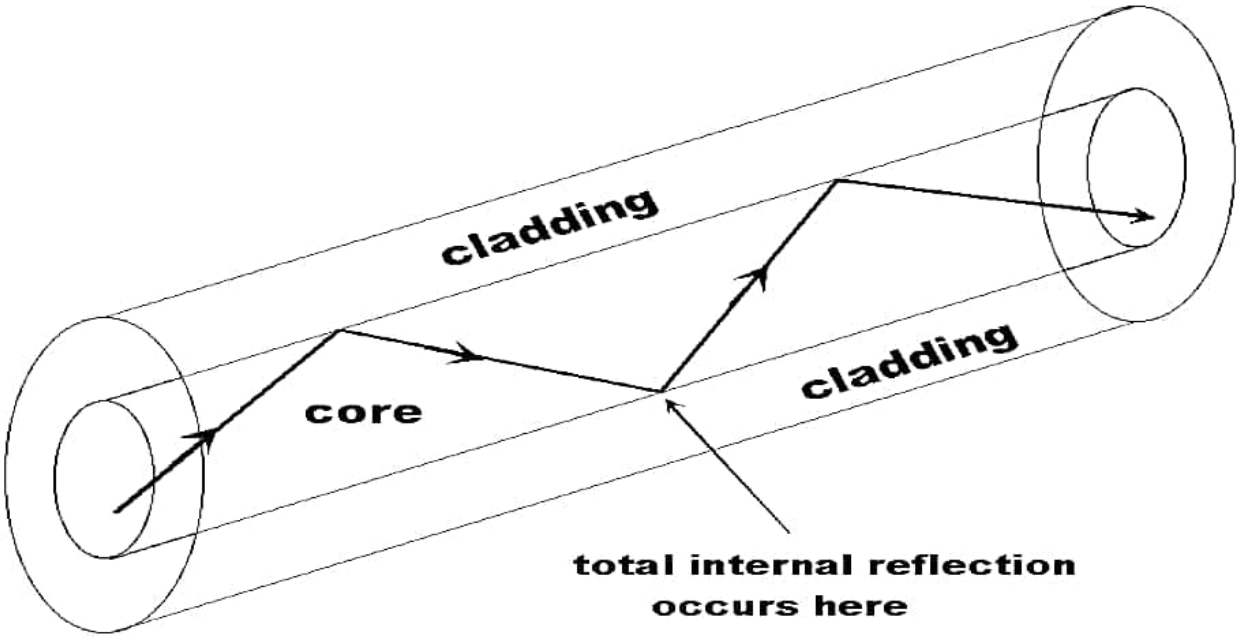

Fig.2.4 A fiber passing light with TIR

The refractive index of the microstructured cladding in PCFs exhibits a wavelength dependency very different from pure silica. The strong wavelength dependence of the refractive index allows design of endlessly single-moded fibers, where only a single mode is supported regardless of optical wavelength. It is possible to alter the dispersion properties of the fibers, thereby making it possible to design fibers with an anomalous dispersion at visible wavelengths. Due to specific control of the refractive index profile, fibers with extremely large mode field diameters are made possible [36]. This supports high beam quality fiber guidance, amplification and lasing.

2.5.2 Photonic Band Gap

Photonic band gap fibers (PBGFs) are so called because the cladding with PC structure can exhibit photonic band gaps (PBG) at optical frequencies [37]. Light whose frequency falls into the band gaps would be totally trapped in the core even when the refractive index of the core is lower than that of the cladding. This low- index core ensures that there is no possibility of wave guiding by TIR. The light guiding can only be achieved by the PBG property. The first PBGF was demonstrated in 1998[38], where an extra hole was introduced to the solid core area to lower the effective index of the core. In PBG guidance mechanism, hallow core guidance becomes possible [39]. Single-mode hollow core waveguides have a multitude of potential applications such as ultrahigh-power transmission, guiding of atoms and particles and gas-based nonlinear optics [40].

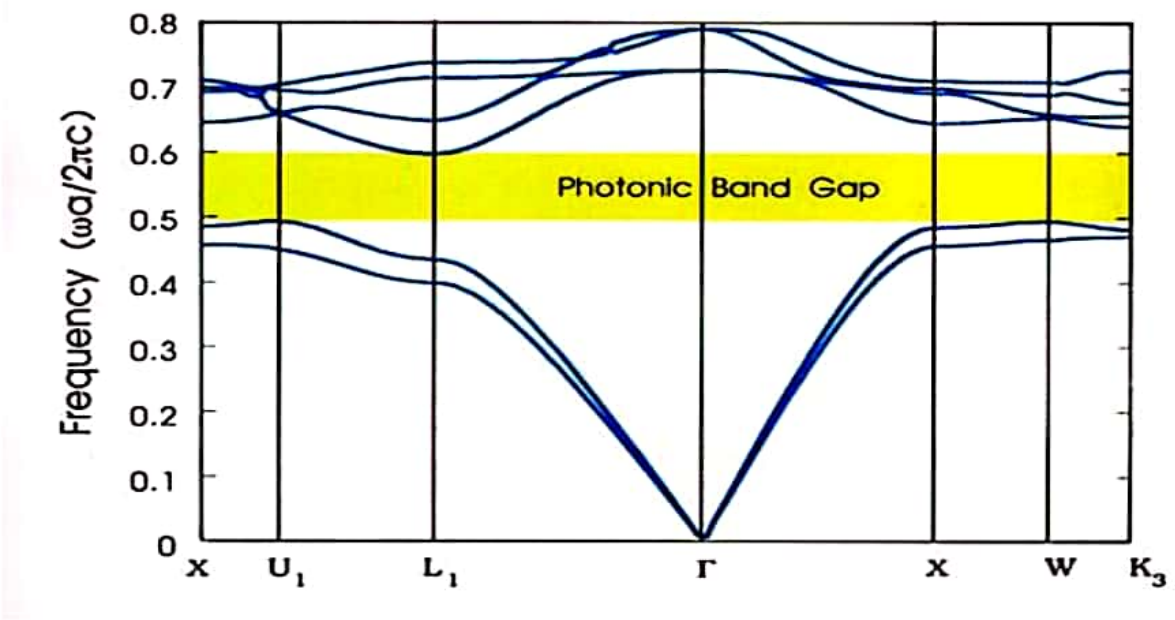

Fig.2.5 Photonic Band-gap

PBGFs seem obviously interesting because of the new guidance mechanism, however TIR PCFs also display unique and useful properties. This thesis will focus on TIR PCFs. Thus in the following discussion of this thesis, the term PCFs refers to silica TIR PCFs unless noted otherwise.

2.6 Properties of PCF

This section presents properties of PCF related to the scope of this thesis. .Properties of PCF includes refractive index, chromatic dispersion, bi-refringence, confinement loss, effective area and dispersion slope.

2.6.1 Refractive Index

In optics, the refractive index or index of refraction of a material is a dimensionless number that describes how light propagates through that medium. It is defined as

$$n \equiv \frac{c}{v}$$

where c is the speed of light in vacuum and v is the phase velocity of light in the medium. For example, the refractive index of water is 1.333, meaning that light travels 1.333 times slower in water than in the vacuum.

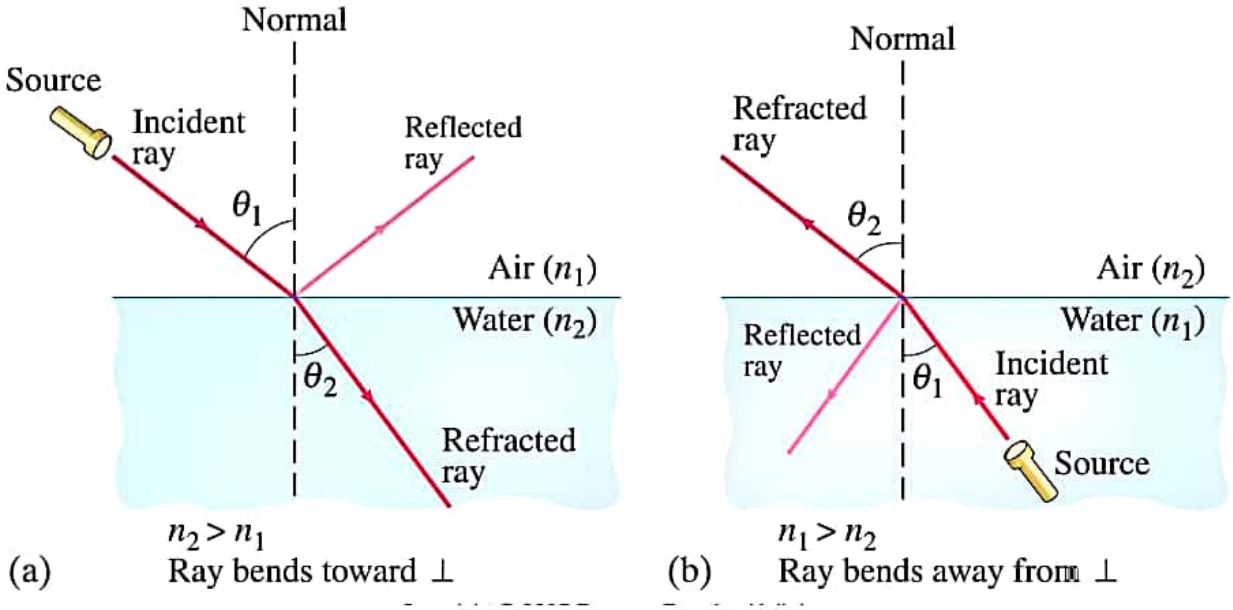

Fig.2.6 Refractive Index

The refractive index determines how much the path of light is bent, or refracted, when entering a material. This is the first documented use of refractive indices and is described by Snell's law of refraction, $n_i \sin\theta_i = n_r \sin\theta_r$, where θ_i and θ_r are the angles of incidence and refraction, respectively, of a ray crossing the interface between two media with refractive indices n_i and n_r. The refractive indices also determine the amount of light that is reflected when reaching the interface, as well as the critical angle for total internal reflection and Brewster's angle.

2.6.2 Chromatic Dispersion

Material dispersion is the phenomena whereby materials cause a "bundle" of light to spread out as it propagates. We know that a laser pulse, while almost monochromatic, actually contains a continuum of wavelengths in a small range. The index of refraction of a material is dependent on the wavelength, so each frequency component actually travels at a slightly different speed. As the distance increases, the pulse becomes broader as a result. Material dispersion limits how much data can be sent, as the pulses will overlap and information will be lost.

$$\tau_g = \frac{L}{c}\left[n - \lambda\frac{dn}{d\lambda}\right] \tag{2.2}$$

Here τ_g is the group delay and L is the propagation distance. From this the material dispersion can be calculated and that is-

$$D = -\frac{\lambda}{c}\frac{d^2\lambda}{d\lambda^2} \tag{2.3}$$

On the other hand waveguide dispersion strongly depends on the silica-air structure itself and can be altered significantly by modulating some parameters like geometry of the air-holes, pitch, and air-hole diameters [41]. Hence, the waveguide dispersion, of PCF is related to those additional design parameters and by optimizing these parameters, suitable dispersion properties can be achieved for dispersion compensation of single mode fiber. It should be pointed out that chromatic dispersion, is algebraic sum of material dispersion and waveguide dispersion upon which material dispersion is calculated from Sellmeier equation and is directly included in the FEM calculation process[41].

Material dispersion + Waveguide dispersion = Chromatic dispersion

Chromatic dispersion is one of the most fundamental characteristics of optical fiber. Dispersion means the variation of velocity with the change of refractive index. The pulse is broadened mostly because of this factor. Dispersion limits the maximum transmission distance and the bit rate in optical fiber communication [42]. The chromatic dispersion in ps/(nm.km) is easily calculated from the following equation

$$D = -\frac{\lambda}{c}\frac{d^2\,\mathrm{Re}[n_{eff}]}{d\lambda^2} \tag{2.4}$$

Where, $\mathrm{Re}[n_{\mathrm{eff}}]$ is the real part of effective refractive index n_{eff} , λ is the wavelength, c is the velocity of light in vacuum. A PCF with negative dispersion coefficient can be used to minimize the positive dispersion of fiber. A high negative dispersion fiber is necessary for dispersion compensation.

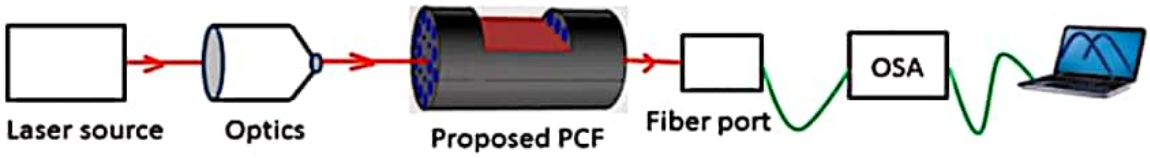

Fig.2.7Figure illustrating dispersion phenomena in optical systems

2.6.3 Birefringence

Real optical fibers including PCFs exhibit considerable variation in core shapes along length of the fiber. Beside this, cylindrical symmetry of a fiber may also be destroyed when it experience

a non-uniform stress [43].When uniformity of the optical fibers is broken, they acquire birefringence which leads to periodic power exchange between the two orthogonal components. This period as shown in Fig.2.5 is called the beat length of the fiber [44].Because of this effect, a linearly polarized light remains the same only alone the principal axes. Otherwise, the state of polarization changes along the fiber length from linear to elliptical and again back to linear state from the elliptical one over the beat length. When, in a fiber, stress applying parts or symmetry breaking parts is added intentionally so that the birefringence is no longer governed by the random core size and shape, it is called a PM fiber. In such a case, intentionally introduced birefringence weakens the random polarization effect. The typical value of birefringence is of the order 10^{-4} for conventional PM fibers. The birefringence is calculated by the following equation where B represents the birefringence.

$$B = \left| n_{eff}^{x} - n_{eff}^{y} \right| \tag{2.5}$$

Where n_{eff}^{x} and n_{eff}^{y} are fundamental effective refractive indices of each fundamental mode.

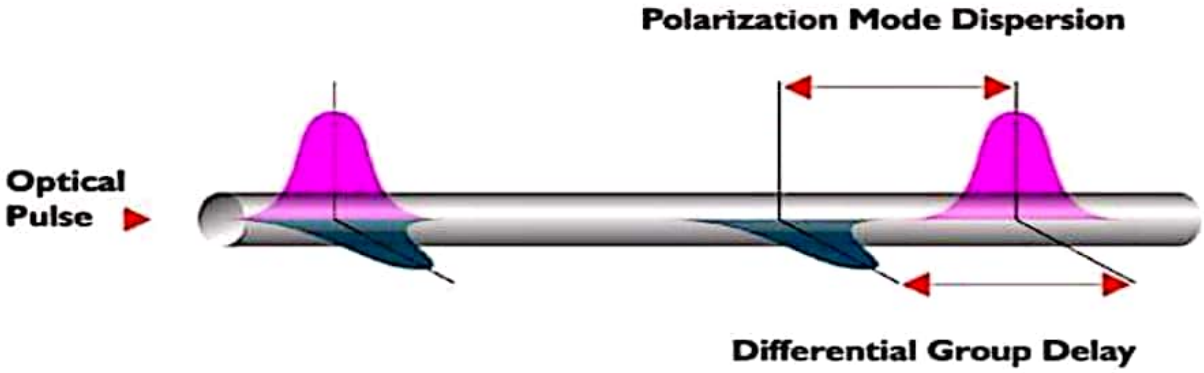

Fig.2.8 Polarization state over one beat length in a birefringent fiber.

2.6.4 Confinement Loss

The confinement loss is a phenomenon whereby part of the guided light penetrates to the cladding region and thereby causes signal degradation. Similar to the conventional fibers, IG-PCFs guide light based on the TIR mechanism and supports three kinds of modes namely- the guided mode, the radiation mode, and the leaky modes [45]. Among these modes, confinement loss is treated as the loss of leaky modes. In PCF, the core and the cladding effective refractive indexes are the same except that there are a finite number of air-holes in the cladding. As a result, guided modes in PCFs are intrinsically leaky. There will be no confinement losses in PCFs if and only if there is infinite number of air-holes in the cladding [46]. Theoretically, confinement losses in PCFs arise from the finite size of the cladding. A fiber with infinite cladding can be

free from confinement losses. This loss depends on the size of the core, air-hole dimension, pitch, and number of rings in the cladding. Fig.2.9 illustrates confinement losses in PCFs. It shows that the guiding light is penetrating to the cladding region through between air-holes. Confinement loss plays a great role in sensors performance calculation. We can calculate sensors confinement loss by using following equation

$$\alpha(dB/cm) = 8.686 \times k_o \, \mathrm{Im}(n_{eff}) \times 10^4 \tag{2.6}$$

Here, $\mathrm{Im}(n_{eff})$ is imaginary part of mode index, $k_o = \frac{2\pi}{\lambda}$ is wave number where λ is operating wavelength.

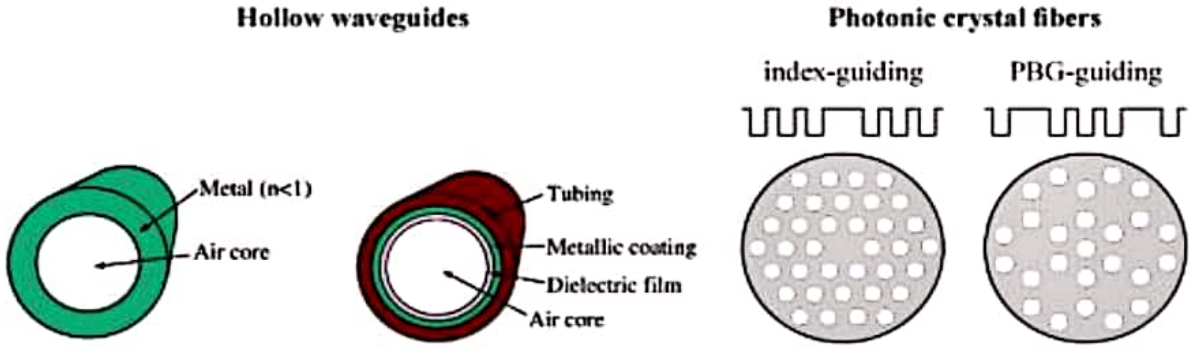

Fig.2.9 Confinement losses in index-guiding photonic crystal fibers.

2.6.5 Effective Area

Fig. 2.10 shows the intensity distribution of a light beam inside a fiber. Such a Gaussian distribution is often used to represent light distribution of optical fibers as it closely assumes the experimental profile [47]. The effective area A_{eff} is calculated as follows-

$$A_{eff} = \frac{\left(\iint |E|^2 dxdy\right)^2}{\iint |E|^4 dxdy} \tag{2.7}$$

Where A_{eff} is in μm^2 and E is the electric field amplitude in the medium.

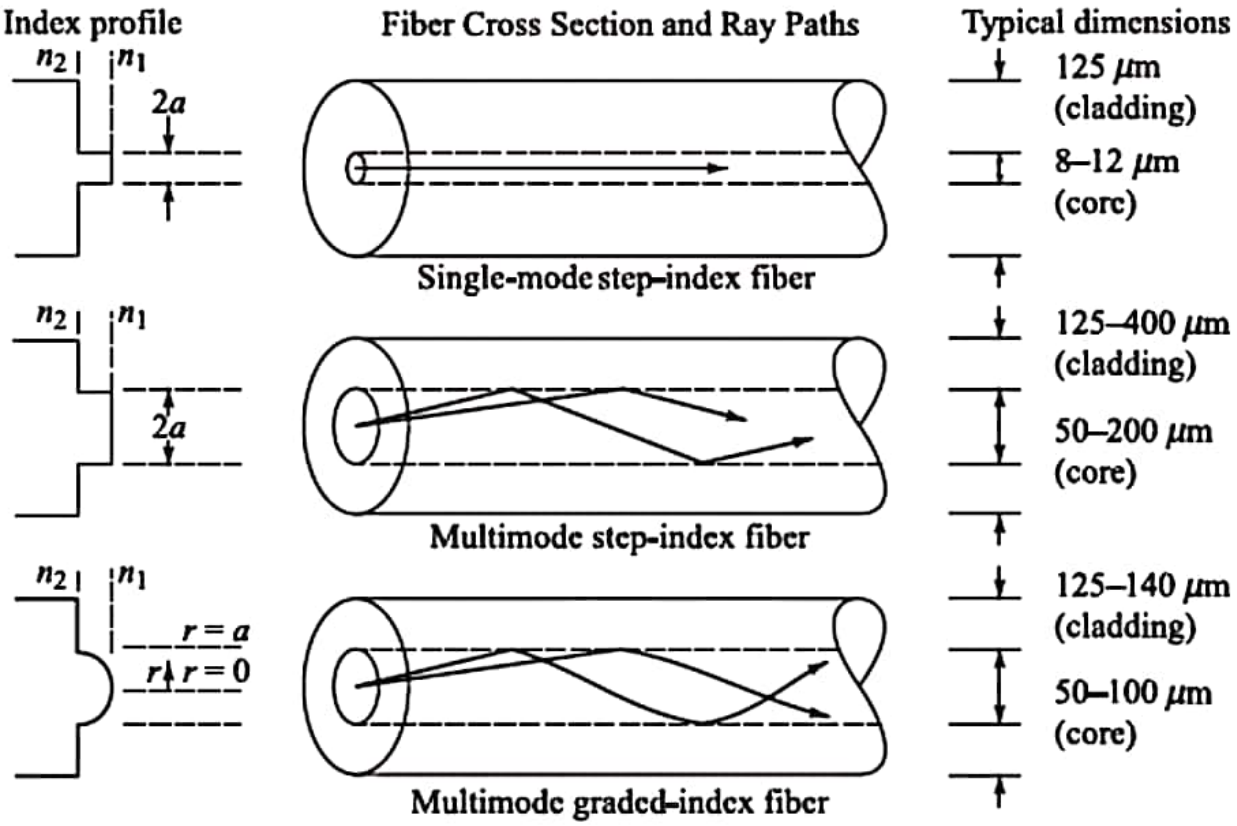

Fig.2.10 Figure explaining mode field diameter and effective area of optical fibers (step index profile). Red curve shows the Gaussian intensity profile.

The effective area or simply the effective area is the area where the beam intensity drops to 13.5% of the maximum value and the diameter of which is called the mode field diameter (MFD) and can be calculated directly from the electric field distribution by using the Petermann II definition [48].

2.7 Summary

Photonic crystal fiber (PCF) basics and their properties are briefly discussed in this chapter. For ease of understanding, we try to add a figure where the required equations are needed .

Chapter 3

Methodology and Simulation

3.1 Introduction

The design of the proposed sensor(Round Core of Optical Fiber) is presented in detail in this chapter. The theoretical description of the model is elucidated in terms of its numerical characterization in order to match real life operations as well as its performance metrics. All numerical tools used in the implementation of these are included in this chapter.

3.2 Description of Different Methods

The transfer-matrix method is used in optics and acoustics to evaluate the propagation of electromagnetic or acoustic waves through a layered medium. The reflection of light from a single interface between two media is described by the Fresnel equations. When there are multiple interfaces, the reflections themselves are also partially transmitted and then partially reflected. These reflections can affect destructively or constructively depending on the precise path length. The overall reflection of a layer structure is the sum of an infinite number of reflections, which is clumsy to calculate . According to Maxwell's equations, there are simple continuity conditions for the electric field across boundaries from one medium to the next; the transfer-matrix method is founded on that element. The final step of the method involves converting the system matrix back into reflection and transmission coefficients.

Plane wave expansion method is a computational technique in electromagnetics to solve the Maxwell's equations by formulating an eigen value problem out of the equation. As this method is used in solving band structure of specific photonic crystal geometries and band structure is related to dispersion relation. This method is popular for designing the photonic crystal fibers . Plane wave method is useful in calculating modal solutions of Maxwell's equations. It is used in computing over an inhomogeneous or periodic geometry. It is fully vectorial method that is applied directly to the fiber design. In [96] particular knowledge about the solution is not required, when characteristic width and center of each chosen with localized function approach.

Finite Element method (FEM) is an arithmetic technique for finding estimated solutions to boundary value problems for partial differential equations. Finite elements are used which are the subdivision of a whole problem domain into simpler parts. By minimizing an associated error function, it uses also variational methods to solve the problem. A complex equation is

approximated over a larger domain, by connecting many simple element equations over many small sub-domains, named finite elements in FEM [49]. This discrete element idealization was a different approach to the solution of continuum mechanics problems; hence the terminology finite element method was created.

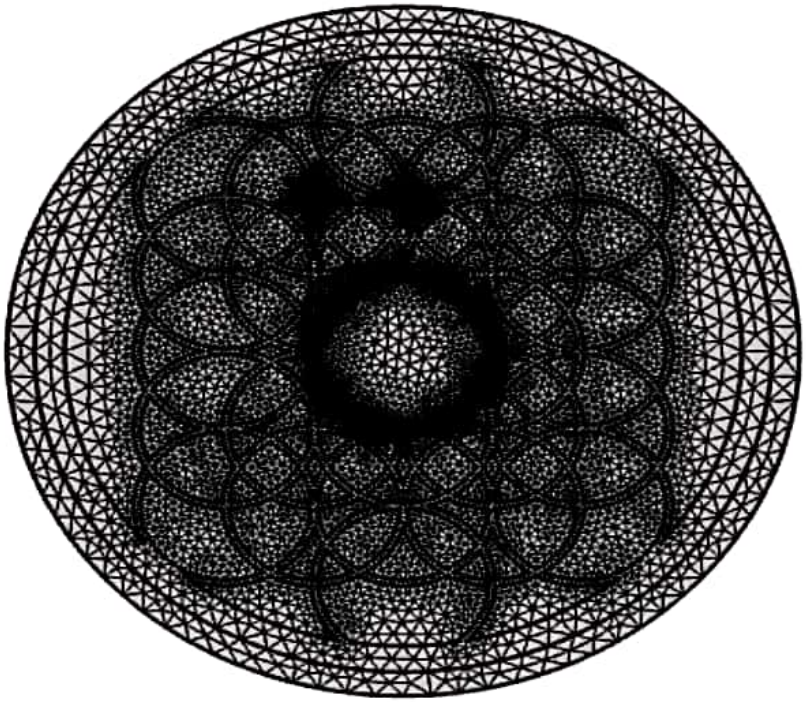

Fig.3.1 The Finite Element Idealization

Fig.3.1 is indicated that models for both continuous structures and frame structures were modeled as a system of elements interconnected at joints or nodes. In many researches on structural analysis, it has realized that the potential of solving problems in continuum mechanics by using discrete elements.

The Finite-Difference Time-Domain method (FDTD) is one of the most popular techniques for the solution of electromagnetic problems now days. It has been successfully applied to an extremely wide variety of problems, such as scattering from metal objects and dielectrics, antennas, micro-strip circuits, and electromagnetic absorption in the human body exposed to radiation. The FDTD method is extremely simple, even for programming a three -dimensional code. Since it is a time-domain method, FDTD solutions can cover a wide frequency range with a single simulation run. Nonlinear or time-varying components are more easily undertook in time-domain [50].

3.3 Finite Element Method

In this thesis, finite element method (FEM) [51] is used as a numerical tool to investigate the propagation characteristics of modes. FEM allows the solution of a large class of partial

differential equations without any limitation by geometry. Furthermore, the use of FEM necessitates the division of the PCF cross section into homogenous subspaces (mesh) within each Maxwell's equations, accounting for adjacent subspaces. For fibers, as in this case, the use of triangular subspaces provides a good approximation for it's circulate nature [52]

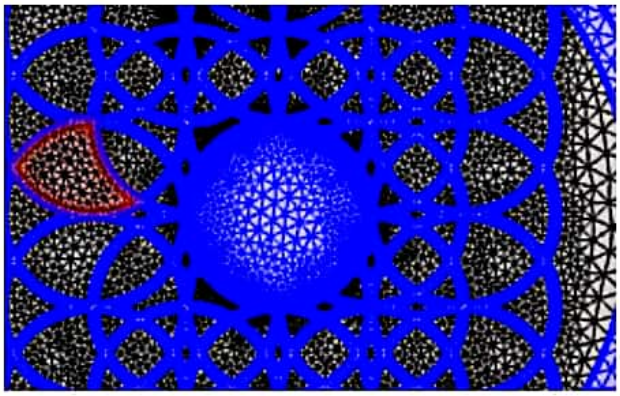

Fig.3.2 FEM mesh

Considering the unique structures of PCFs a full vector FEM formulation would be required study wave propagation through fibers with arbitrary air filling fraction. Full vectorial FEM incorporates an isotropic perfectly matches layers (PML) enabling one to solve for as many modes as desired in a single run without iterating[52]. Analysis of leaky modes is also possible with PMLs. As such, both dispersion and loss properties can be determined in a single run. In the case of propagation mode computation, FEM creates a matrix that numerically approximates the partial differential operator of the problem transforming it into numerical Eigen-value problem, which is then solved using numerical algebra techniques.

3.4 Proposition for the Use of FEM

Each of the methods mentioned above has specific advantages when analyzing micro-structured fibers . For specific advantage, specific method is used. In this thesis, FEM method is used. This method presents accurate representation of complex geometry. Finite element method is an addition of divergent material properties. It is an easy representation of the total solution. FEM is more suited to solve complex non-linear problems [53]. Transfer Matrix method is numerically unusable in the presence of layer with strong attenuation. It is not preferable for calculate the characteristics of the proposed model.

The finite-difference method (FDM) is much simpler to implement, but the structured grid makes it not as efficient as the finite-element method. Finite element methods are better on irregular domains, especially when boundary conditions involve. The main advantage of the Finite Element Method over the Finite Difference Method is its ability to deal with complex 2D

or 3D domains [48]. When the region is a rectangle or a union of rectangles, FDM can be used. On the other hand, when the problem needs local mesh refinement FEM outperform the finite difference method. The proposed model has to be fulfilled the boundary condition as well as mesh refinement, so the FEM is more appropriate method than finite difference method. At [53], in Plane Wave method sometimes spurious modes appear and the number of the plane waves used in the problem. This is both time consuming and complex in memory requirements. Alternatives include methods using FEM which is simpler, and model transients. If implemented correctly, spurious solutions are avoided. PWM is less efficient when index contrast is high or when metals are fused. It cannot be used for scattering analysis. There is a used non-localized basis function in PWM [47]. These are hard to parallelize efficiently. The offered model uses fused silica as material but PWM is less efficient when a fused metal is used. In this perspective FEM is more applicable than PWM for this thesis. Furthermore, scattering analysis is necessary which is possible in FEM rather than PWM.

Commercial finite element software package COMSOL is used to calculate solutions, where numerical errors occur as the wave propagation is founded. The effect of several numerical parameters are examined and concluded that reducing the element size decreases the overall error of the solution. This also helps reduce numerical oscillations if present. Increasing the element order also improved the solution [54]. The time stepping algorithm was found to have a strong connection to the element size. The maximum time step depends strongly on the minimum element size. The FEM can solve inhomogeneous domains with relative ease compared to homogeneous domains, which may be an advantage over other methods. The dispersion analysis for the FEM is usually accompanied by using uniform structured meshes because specific numerical wave numbers can be solved to strongly show the dispersion behaviors of the FEM meshes and elements under consideration. However, one of the major reasons for using FEM is this method's ability to model geometrically and compositionally complex problems [55]. Since the hexagonal mesh has the smallest numerical dispersion, it is reasonable to assume that the regular triangles are the best shapes in terms of numerical dispersion, and any triangle that is close to being equilateral would introduce small numerical dispersion. This is reliable with the classic issue of the quality of the element shapes, which basically states that the regular triangles are of the best quality [55]. In this case FEM is more significant than other methods.

3.5 Implementation of FEM on PCFs

The study of hybrid mode and polarization dependent wave propagation requires a full vectorial analysis. Consider an optical waveguide with an arbitrary cross section in the x-y plane, has a full vectorial wave equation derived from Maxwell's equations in the form of

$$\nabla \times ([p] \nabla \times \varphi) - k_0^2 [q] \varphi = 0 \tag{3.1}$$

3.6 Perfectly Matched Layer

These are additional spaces/domains that do not reflect incident radiation rather absorbs them. As part of the model, it's specified to be made of a different absorbing material of varied thickness. This absorbing material must have matching an isotropic permeability and permittivity with the physical medium outside the PML such that there are no reflections. Maxwell's equations can be used to formulate the PML by introducing a complex valued coordinate transform under the additional requirement that the wave impedance should remain unaffected.

3.7 Effective Refractive Index

In homogeneous transparent media, the refractive index n can be used to quantify the phase change per unit length: that phase change is n times higher than it would be in vacuum. The effective refractive index n_{eff} has the same meaning for light propagation in a waveguide and depends not only on the wavelength but also on the mode in which the light propagates. The effective index may be a complex quantity in which case the imaginary part describes gain or loss [56].

3.8 Numerical Tools

There are two numerical tools used in this thesis. They are as follow:

MATLAB® version R2017a is a high-level language and interactive environment for numerical computation, visualization and programming. Its numerical computation capability has been employed in the evaluation of performance parameters such as interrogation modes, birefringence, and confinement loss in this thesis. The tools and built-in math functions allow

multiple approaches in order to arrive at a solution faster as opposed to spreadsheets or traditional programming languages [57].

COMSOL Multi-physics is a powerful software package that can perform eigen-frequency and modal analysis. COMSOL Multi physics employs the proven finite element method (FEM). The software runs the finite element analysis to get adaptive meshing and error control using a variety of numerical solvers. With this software you can design Photonic crystal fibers easily by defining the sub-domains and boundary conditions with correct parameters and also you can solve the problems for both electric field and magnetic field. For designing the structure COMSOL Multi-physics version 5.5 is used.

3.9 Summary

In this chapter, we briefly discuss various simulation methods, with relative ease compared to other homogeneous domains, FEM can solve in homogeneous domain. In addition, the use of uniform standardized mesh is followed by FEM. Since FEM is essential than other methods, on both the PCFs, we implement FEM. In addition to this, in this chapter, we address PML, effective refractive index and numerical instruments..

Chapter 4

Design and Result Analysis of Round Core Optical fibre PCF with High Sensitivity, Low EML and a low Confinement Loss.

4.1 Introduction

4.2 Structural Design

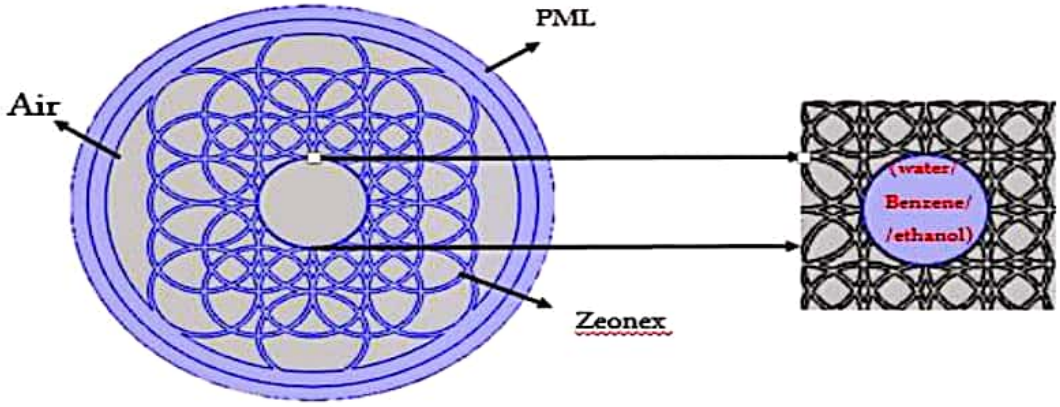

The major goal of the simulation is to determine how much chromatic dispersion is introduced and how much cross-section loss is present when using PCF. For simulation purposes, the following structural parameters were considered:

Perfectly matched layer, t=30, μm core diameter, D=390, μm air hole, d=400, μm, amount of distance that exists between the core and the air hole, R=10, μm core diameter, D=400, μm core diameter. Layer thickness, Z=30,μm , Z=20,μm, Z=10,μm

The sensitivity is the plot to determine how sensitive concerning frequency is. It will allow to observe how sensitive the material is. We later discuss in the graph we plot sensitivity versus frequency to get more idea about the sensitivity of the material especially in a practical point of view(1).

$$r = \frac{n_r}{n_{rff}} \times X \quad \text{----------(1)}$$

The refractive index of the target that will be sensed. n_{eff} effective refractive index of the mode in the guided precisely in addition to this, it can also be used for the representation of the interaction of light(1).

The effective material loss is calculated by the equation .

$$A_{eff} = \frac{\left(\iint |E|^2 dxdy\right)^2}{\iint |E|^4 dxdy} \text{ ---------- (2)}$$

Confinement loss is the process where by some guided parts of the lights penetrates into the cladding region. When this happens, it causes the degradation of the signal which is somehow similar to fibers convention. The photonic crystal fibers guides the based light on its total internal reflection (TIR). In the photonic crystal fibers the cladding have various holes due to the guide's modes in photonic fibers. This can theoretically be seen, when it arises from various size of the cladding. From this it can be seen that sometimes the fiber has so many various claddings to avoid the confinement losses, but the size of the core in the air hole depends on it. Here, $\mathrm{Im}(n_{eff})$ is imaginary part of mode index, $k_o = \frac{2\pi}{\lambda}$ is wave number where λ is operating wavelengt, To calculate the sensor for confinement loss, simply use this equation

$$\mathrm{L_C} = (\frac{4\pi f}{c})\,\mathrm{Im}(n_{eff}), cm^{-1} \text{ ---------- (3)}$$

By using this equation, we can determine the birefringence.

$$B = \left|n_{eff}^{x} - n_{eff}^{y}\right| \text{ ---------- (4)}$$

Where n_{eff}^{x} and n_{eff}^{y} are fundamental effective refractive indices is frequently evaluated as the greatest contrast between refractive indices and
Each fundamental mode.

$$n = \frac{c}{v} \text{ ---------- (5)}$$

From equation (5) When the frequency of light in the vacuum is inversely proportional to the velocity of light. Examples are the speed of the light in the vacuum (c) and the speed of the light phase (c) (v). Well, it's for the moment, anyway. The water refractive record shows that light is 1.33 times slower in the water than in the vacuum.

$$\tau_g = \frac{L}{c}\left[n - \lambda\frac{dn}{d\lambda}\right] \text{ ---------- (6)}$$

L is the propagation distance, and τg is the group delay. Once we have that, we can calculate the material dispersion.

$$\beta_2 = \frac{2}{c}\frac{dn_{eff}}{d\omega} + \frac{\omega}{c}\frac{d^2 n_{eff}}{d\omega^2} \quad \text{---------- (7)}$$

From equation (7) the β_2 constant is a propagation constant.The velocity of light in a vacuum and is denoted by c, Re[n_{eff}] is the real part of the effective and ω.

is the omega, c is the speed of light in vacuum, to limit the positive dispersion of fiber, a PCF with a negative dispersion coefficient can be used. For proper dispersion compensation, a high negative dispersion fiber is needed..

From equation (8) Convincing refractive index n_{eff} is where Re (n_{eff})is the is the core, while λ is the frequency, and c is the speed of light in a vacuum. To reduce the positive dispersion of fiber, a PCF with a negative dispersion coefficient can be used. dispersion compensation is greatly affected by a high negative dispersion fiber.

$$D = -\frac{\lambda}{c}\frac{d^2 \mathrm{Re}[n_{eff}]}{d\lambda^2} \quad \text{---------- (8)}$$

From equation (9) Re (n_{eff})is the is the real part of of compelling refractive index neff , f is the frequency, c is the speed of light in vacuum. The numerical aperture of the optical frame is derived by referencing the shaft's refractive index, as well as the sine of the pivot where the beams can be transmitted using mathematical equations. The numerical aperture is a material property that can be determined from this calculation..

$$NA = \frac{1}{\sqrt{1 + \frac{\pi n_{eff} f^2}{c^2}}} \quad \text{---------- (9)}$$

4.3 Simulation and Performance Analysis

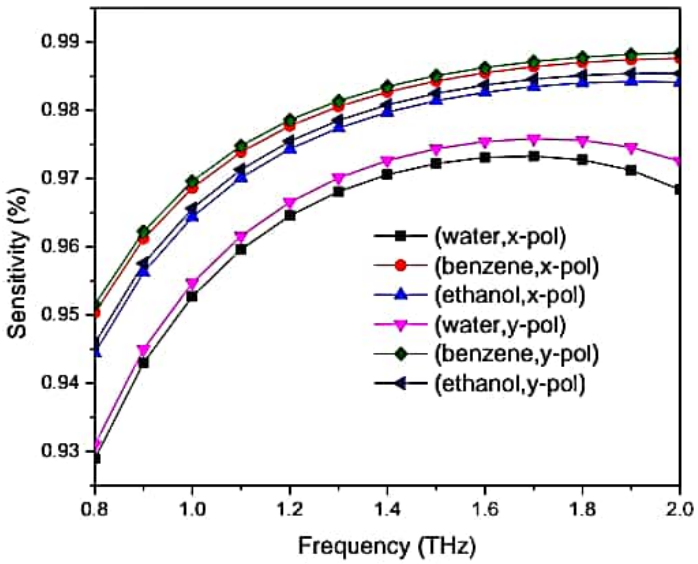

Fig 4.2: sensitivity of ethanol, benzene, and water versus frequency with varying 30 thickness

From fig 4.2, by increasing the frequency boosts sensitivity. Also, when D=390 μm, maximum sensitivity is observed. Note that, D = 390 μm is the maximum frequency of the core and increment above this limit will overlap the core with the cladding. A side effect of our research was to investigate further the sensing capability. To do this, we changed the frequency and we readings found that when we lower the core, sensitivity goes down. Therefore, to minimize manufacturing difficulties we should keep the core and cladding separate when fabricating flexible structures. implies that the core accommodate a more significant volume of the chemical to be sensed allowing more interaction between the analyte and the fiber core thereby increasing the sensitivity Hence it can be concluded that sensitivities in our design was found as 98.7% .

For our design the layer thickness at Z=30 ,um. It is only dependent on the real part of (RI), and so thickness changes have no effect on variation in sensitivity, to make sure everything else is perfect we performed the convergent test as demonstrated in Fig.4.3, Fig.4.4, to determine the thickness shown in those figures.

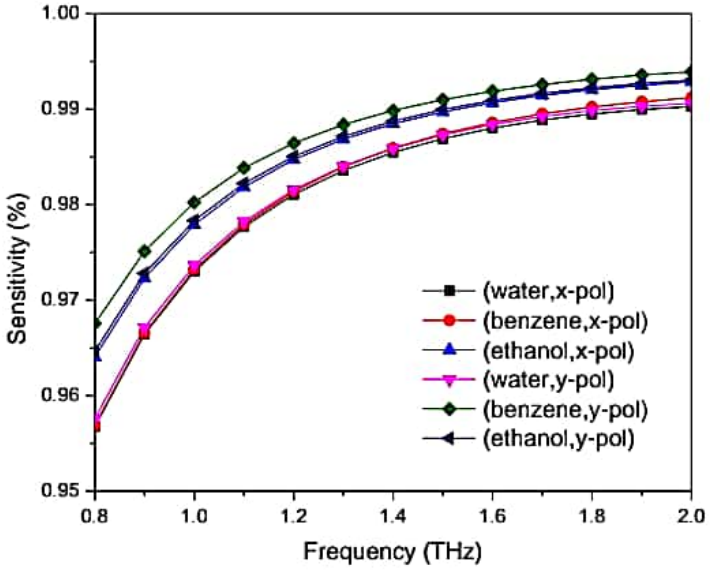

Fig 4.3: sensitivity of ethanol, benzene, and water versus frequency with varying 20 thickness

From fig4.3, the sensitivity increases when the frequency is increased.. Maximum sensitivity is also observed when D, is equal to 390, µm. Even if you increase the frequency of the core above D = 390 µm, there will be closed with the cladding. A byproduct of our research was to further explore the ability to sense. To accomplish this, we lowered the core frequency and the readings show that sensitivity declines when the core is lowered. This makes it easier to manufacture flexible structures because the core and the cladding are kept separate when we make them. alludes to the fact that the core accommodates a larger volume of the chemical to be sensed, which encourages a higher concentration of the analyte, and so the interaction between the analyte and the fiber core increases Thus, it can be deduced that our design had a high sensitivity of 99.3 %.

At Z=20 um, our design's layer thickness is We performed the convergent test as demonstrated in Figure 4.2, Figure 4.4, to determine the thickness of those figures.

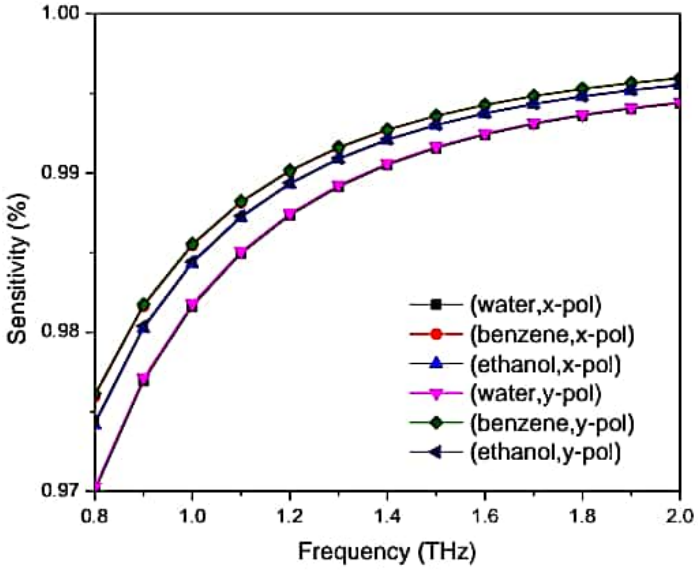

Fig 4.4: sensitivity of ethanol, benzene, and water versus frequency with varying 10 thickness

From fig 4.4, the sensitivity increases when the frequency is increased. And in figure 4 the sensitivity is improved more than fig 3 and fig 2. To have the maximum sensitivity, the values of D=390, um. There will be overlap with the cladding even if you increase the frequency of the core above D = 390 μm. We discovered a previously unknown ability that allowed us to seek out other abilities. By lowering the core frequency, we found that sensitivity is reduced. Since the core and the cladding are kept separate when we manufacture them, the structures are flexible. in addition to this, because the core is bigger, the capacity to accommodate a higher concentration of the chemical to be sensed means that the quantity of the analyte must be greater, thus increasing the degree of interaction between the analyte and the fiber core. Using this logic, it follows that our design had a 99.5% response.

Our design's layer thickness is at Z=10 um ,it's the higher one . As shown in Figure 4.2, Figure 4.3, we conducted the convergent test to discover the thickness of those figures.

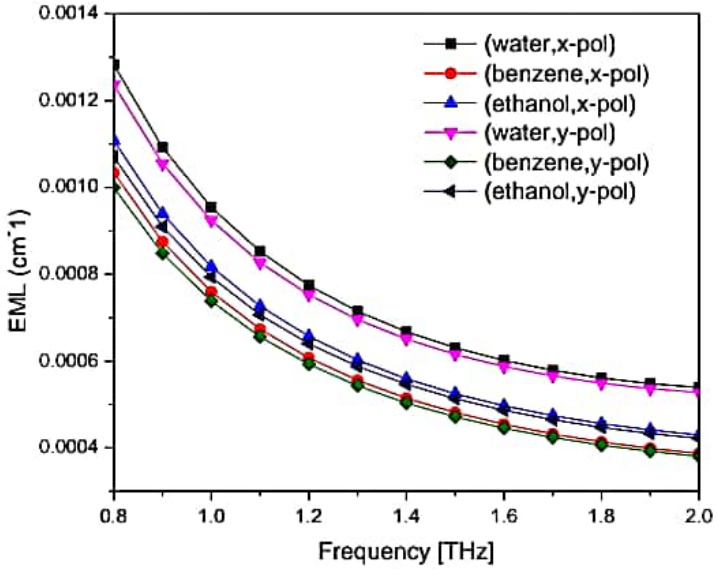

Fig 4.5: Effective material loss of ethanol, benzene, and water versus frequency.

From fig 4.5, the effect of varying core on EML can be observed by varying the analyte It can be seen that with increased frequency, the amount of EML increases. One may observe that the higher the frequency that satisfies the theoretical condition for calculating EML, the higher the EML rises. From Fig. 9, in addition, it is obvious thatthe lowest EML ever realized in a PCF-based waveguide is at the optimal design conditions, the range of frequencies starts at 0.8 to 2 THz , so the value of EML become 0.0004 cm^1 .

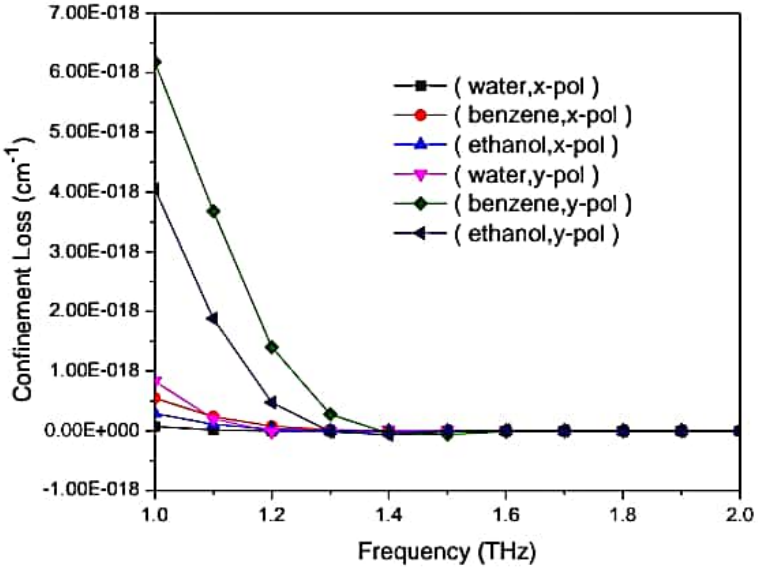

Fig 4.6: confinement loss ethanol, benzene, and water versus frequency..

. From Fig. 4.6 ,it Marks the difference in the type of confinement loss for different analytes. It appears that as the frequency of use increases, the reduction in losses due to confinement becomes more noticeable, the frequency increment causing a tightening of the mode fields in the round core core region. The results may be due to the fact that the more frequently a signal is transmitted, the more constricted it becomes, thus lowering the overall Autocorrelation thus the confinement loss for water($1\times10^{-21}cm^{-1}$, $4.4\times10^{-21}cm^{-1}$),ethanol ($1.06\times10^{-20}cm^{-1}$, $5.8\times10^{-21}cm^{-1}$) and benzene ($2.3\times10^{-20}cm^{-1}$, $5.8\times10^{-21}cm^{-1}$) respectively with x and y polarization .

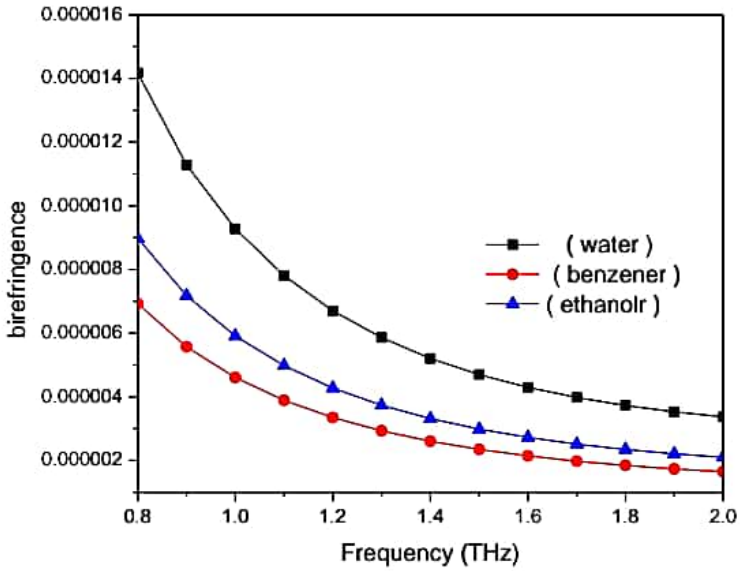

Fig 4.7: Birefringence of ethanol, benzene, and water versus frequency.

From fig 4.7, the Sensor sensing performance is improved by the polarization maintaining property of a fiber. There are two distinct modes: x polarization mode, and y polarization mode. As shown in fig.4.7. for different analyte variation, the property of birefringence holds. As the frequency increases, birefringence decreases. In order to decrease the index difference between the polarization modes, the frequency must increase. The birefringence that is obtained when the design parameters are optimally selected is water: 0.000004, ethanol 0.000003 and benzene 0.000004. Please be aware that it is possible to increase the birefringence even further by either reducing the core diameter or diameter of the core's outer layer.

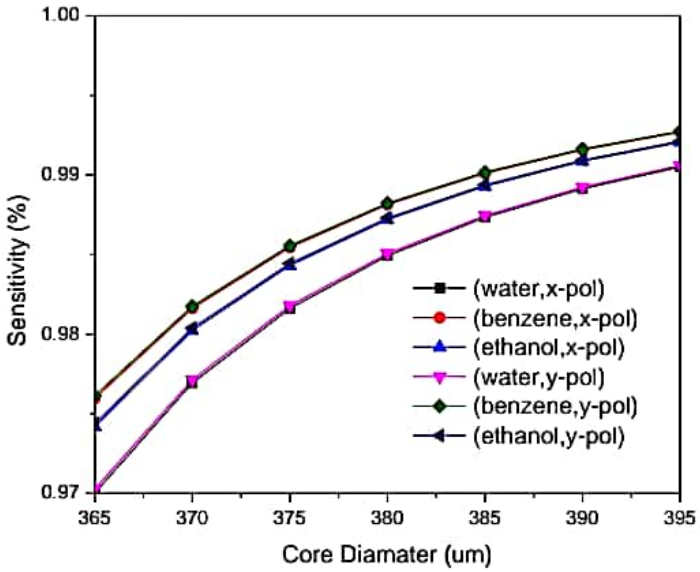

Fig: 4.8 core diameter of ethanol, benzene, and water versus core sensitivity. (%)

From fig 4.8, we illustrates the relationship between varying sensitivity and core diameter, which is important since additional air holes are used around the core to boost sensitivity. This is demonstrated by the fact that sensitivity increases as core diameter increases. This can be explained by the fact that, when we increase the core diameter, we are faced with the present of an electomagnetic field which causes sensitivity to increase significantly which can be seen from our graph the core diameter at 365 to 395, um .

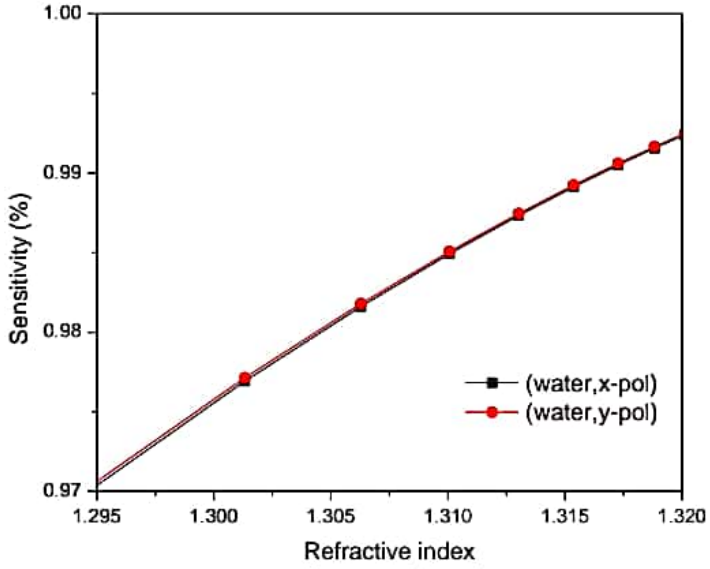

Fig. 4.9. sensitivity of ethanol, benzene, and water versus of refractive index

From fig 4.9, shows a direct correlation between the sensitivity and the variation of the refractive index (real). And for water, there is a linear correlation between the variation of the core of the cladding air holes and the sensitivity. In order to optimize the core of the cladding air holes, we varied the refractive index and calculated the sensitivity of the water. The slower-moving light occurs when the refractive index is increased.

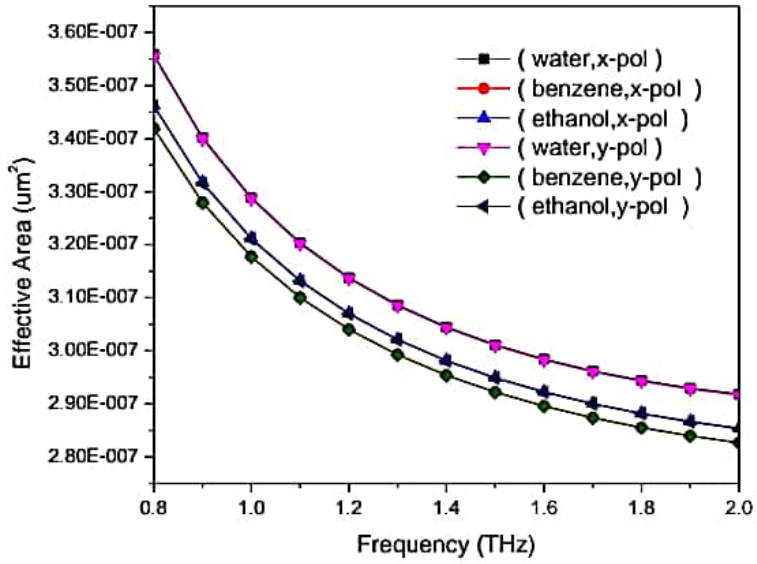

Fig.4.10. Effective Area of ethanol, benzene, and water versus frequency.

From fig 4.10, the proposed PCF cross section depicts the modal effective area for both x and y polarization. What is easily seen is that as the frequency increases, the distribution of the electric field decreases. Since the frequency increases, less light is contained in the porous core region. Effective area is obtained by multiplying the effective area by $3.5\times10^{7}\ um^{2}$. It can be stated that, with regards to communication devices and lasers, a high value of effective area is useful while for fiber non-linearity, a low value works better.

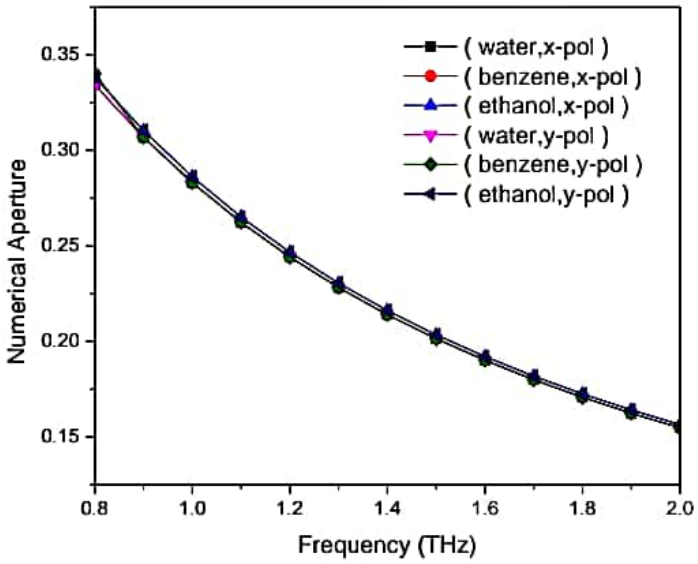

Fig 4.11, Numerical Aperture of ethanol, benzene, and water versus frequency.

From fig 4.11, the NA (numerical aperture) is directly proportional to the frequency. If other factors remain constant, then a relationship can be seen where NA is inversely proportional to frequency, provided other variables remain the same. In other words, the numerical aperture is reduced to compensate for the frequency at which we increase the frequency. Because numerical aperture is proportional to the effective area, and the effective area is proportional to frequency, it should be expected that numerical aperture would be inversely proportional to effective area, which can be seen from our graph the NA at 0.34. .

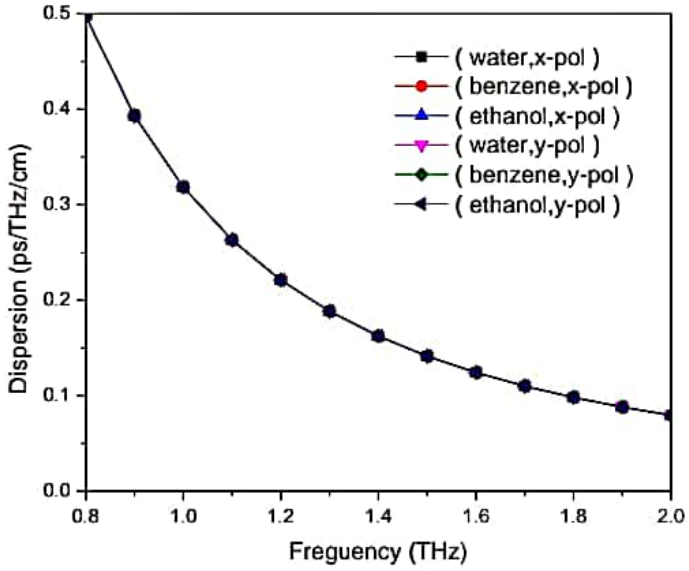

Fig 4.12. Dispersion of ethanol, benzene, and water versus frequency.

From fig 4.12, we describes dispersion in terms of frequency and other design parameters that work best with it. At X-polarization, the dispersion is flatter, which means we select x-polarization as optimal. Under the condition of an ultra-flat- tened dispersion variation of ± 0.50 ps/THz/cm, a 0.50 ps/THz/cm ultra-flat- tened dispersion variation of x-polarization is obtained at a core diameter. As you can see, a PCF dispersion flattened by a suitable factor yields an equal group delay multi-color signal path. Unwanted losses take place in the guided mode when pulses of light travel along the fiber. As most of the polymer materials are lossy, this is the reason.

4.4 Summary

The result analysis is tried to focus for all parameters of the sensors. For ease of understanding, required equations and figures are given. The simulation of the proposed work is performed by COMSOL 5.5 software and plot the figure with the help OriginPro 8.6 64Bit.

Chapter 5

Conclusion and Future Work

5.1 Conclusion

Terahertz-specific fiber is created with a round core and tested for a range of chemical analytes. A simulation study showed that 98.7%, 99.3%, and 99.5% of 10,20,30 layer thickness have a high sensitivity which uses Zeonex as the substrate . Additionally, the sensor shows efficient sensing and a small amount of chromatic dispersion, all while offering extremely low EML and negligible confinement loss. Furthermore, the improved sensing performance is well-suited to it. This PCF can be fabricated using existing fabrication methods. These two factors enable the sensor to exhibit extraordinarily sensitive sensing properties, as well as an unusually wide degree of design flexibility. This new sensor will open up a completely new realm of terahertz research, and it may also have broad-ranging industrial and medical applications. The use of minimal core zone nenoex bridges to generate a low cladding index is demonstrated using a physical model of Zeonex high NA fibres. Several of these types of fibres have been manufactured and the resulting measured properties follow the predictions quite well. NA was 0.34 over a D= 390 ,um. Designs like these will improve both sensor performance and light sensitivity.

5.2 Future work

1. To work with newer types of material
2. To work both core and cladding
3. To work with different types of photonic crystal fiber structure
4. To work with newer types of fabrication method
5. New material can increase the sensitivity.
6. New material can decrease the the EML
7. To work with newer types of material to improve dispersion
8. To work with newer types of material to improve numerical aperture

5.3 Character-wise Comparison Summary

PCFs	Operating region	Sensitivity	Birefringence	EML (cm^{-1})	Dispersion (ps/THz/cm)	Confinement loss
Ref. [58]	1.4 THz	96.8%	0.0154	0.0035	-	6.95×10^{-14}
Ref. [59]	1.6 THz	85.7%	0.005	-	±0.47	1.7×10^{-9}
Ref. [60]	1.8 THz	-	0.086	-	±0.03	3.8×10^{-9}
Ref.[4]	1.8 THz	-	0.039	-	1.07 ± 0.05	
This paper	2 THz	99.5%	0.000014	0.0004	±0.50	1×10^{-21}

References

[1] B. J. Mangan, L. Farr, A. Langford, P. J. Roberts, D. P. Williams, F. Couny, M. Lawman, M. Mason, S. Coupland, R. Flea, H. Sabert, T. A. Birks, J. C. Knight, and P S.Russell, "Low loss (1.7 dB/km) hollow core photonic bandgap fiber," *Optical Fiber Communication Conference and Exhibition, OFC*, PDP24 (Los Angeles, California, USA, 2004).

[2] R. A. Correa, J. C. Knight, "Specialty Fibers: Novel process eases production of hollow core fiber," *Laser Focus World* , Vol. 44, No. 05, May 2008.

[3] Inaba, H., et al, "Optical Fibre Network System for Air-Pollution Monitoring over a Wide Area by Optical Absorption Method", *Electron Letts*. Vol. 15, no.1, pp. 749-751,1979.

[4] M.J. Steel, T.P. White, C.M. de Sterke, R.C. McPhedran, and L.C. Botton, "Symmetry and degeneracy in micro-structured optical fibers," *Opt. Lett.* Vol. **26**, no.9, pp. 488-490, 2001.

[5] A. Bjarklev, J. Broeng, and A. S. Bjarklev, "Photonic Crystal Fibres", *Kluwer Academic Publishers*, USA, 2003.

[6] Dinesh Kumar Prajapati, Ramesh Bharti, "Dispersion analysis of a Hybrid Photonic Crystal Fiber," *International Journal of Recent Research and Review*, vol. 7, no. 2, pp. 118-122, June 2014.

[7] Md. Selim Habib, Md. Samiul Habib, S.M.A. Razzak, "Study on Dual-Concentric-Core Dispersion Compensating Photonic Crystal Fiber," *International Journal of Engineering and Technology*, vol. 4, no. 1, pp. 377-383, Sep. 2012.

[8] R. Buczynski, "Photonic Crystal Fibers," *International School of Semiconducting Compounds*, vol. 106, no. 2, pp. 141-168, Jun. 2004.

[9] P. Russell, "Photonic Crystal Fibers: A Historical Account," *IEEE LEOS NEWSLETTER*, vol. 21, no. 5, pp. 11-15, Oct. 2007.

[10] E. Kretschmann and H. Reather, "Radiative decay of non radiative surface plasmon excited by light." *Z.Naturf.* vol. 23A, pp. 2135-2136, 1968.

[11] E. Kretschmann, "Die Bestimmung optischer Konstanten von Metallen durch Anregung von Oberflachenplasmaschwingugnen." *Z Phys* vol. 241,pp. 313-324,1971.

[12] A. Otto, "Exitation of non-radiative surface plasma waves in silver by the method of frustrated total reflection." *Z Phys* vol. 216, no.1, pp. 398-410, 1968.

[13] B. Liedberg *et al,* "Surface plasmon resonance for gas detection and biosensing." *Lab.Sensors Actuat.* Vol.4,pp. 299-304; (1983).

[14] I. Pockrand *et al* "Surface plasmon spectroscopy of organic monolayer assemblies." *Surface Sci.* 74: 237-244; (1978).

[15] B. Liedberg *et al* "Principles of biosensing with an extended coupling matrix and surface plasmon resonance." *Sensors and Actuators* vol. 11, pp. 63-72,1993.

[16] L. Zhang and D. Uttamchandani, "Optical chemical sensing employing surface plasmon resonance." *Electron Lett.* 23: 1469-1470; (1988).

[17] S. Sjolander and C. Urbaniczky, "Integrated fluid handling system for bio-molecular interaction analysis." *Analytical Chemistry* vol. 63, pp. 2338-2345,1991.

[18] M. Stapelbroek, D. L. Griscom, E. J. Friebele, and G.H. Sigel, "Oxygen-associated trapped-hole centers in high-purity fused silicas," *J. Non-Cryst. Solids* **vol. 32**, pp. 313,1979.

[19] D. L. Griscom, "Defect Structures of glasses," *J. Non-Cryst. Solids* vol. **73**, pp. 51,1985.

[20] G. N. Greaves, "Colour Centers in Vitreous Silica," *Philos. Mag,* B **37**, 447 (1978).

[21] V. B. Neustruev, "Colour centers in germanosilicate glass and optical fibers," *J. Phys.: Condensed Mat.* Vol. **6**, pp.6901, 1994.

[22] J. Lægsgaard, A. Bjarklev, and S. E. B. Libori, "Chromatic dispersion in photonic crystal fibers: fast and accurate scheme for calculation," *J. Opt. Soc. Am.* B **20**, 443 (2003).

[23] K. Tajima, J. Zhou, K. Kurokawa, and K. Nakajima, "Low water peak photonic crystal fibers," *in Proceedings of 29th European Conference on Optical Communication, ECOC'03*, Post deadline paper (Rimini, Italy, 2003), pp. 42.

[24] W. A. Gambling, D. N. Payne, and H. Matsumyra, "Cut-off frequency in radially inhomogeneous single-mode fibre," *Electron. Lett.* Vol. **13**, pp. 139, 1977.

[25] D. Gloge, "Weakly guiding fibers," *Appl. Optics* vol. **10**, pp. 2252, 1971.

[26] D. Marcuse, "Gaussian approximation of the fundamental modes of graded-indexfibers," *J. Opt. Soc. Am.* Vol. **68**, pp.103,1978.

[27] K. F. Klein, R. Arndt, G. Hillrichs, M. Ruetting, M. Veidemanis, R. Dreiskemper, J. Clarkin, and G. Nelson, "UV-Fibers For Applications below 200 nm," *Proceedings of SPIE* **4253**, 42 (2001).

[30] S. Unger, J. Kirchhof, S. Schröter, A. Schwuchow, and H. Frost, "Transmission Behaviour of Silica Core – Fluorine Doped Cladding Fibers in the Visible and Ultraviolet Regions," *Proceedings of SPIE* **4616**, 161 (2002).

[31] J. Vydra and G. Schötz, "Improved all silica fibers for deep UV-applications," *Proceedings of SPIE* ,vol.35, no. 96, pp. 165,1999.

[32] D. L. Griscom and M. Mizuguchi, "Determination of the visible range optical absorption spectrum of proxy radicals in gamma-irradiated fused silica," *J. Non-Cryst. Solids* **239**, 66 (1998).

[33] L. Skuja, K. Tanimura, and N. Itoh, "Correlation between the radiation-induceed intrinsic 4.8 eV optical absorption and 1.9 eV Photoluminescence bands in glassy SiO2," *J. Appl. Phys.* **80**, 3518 (3518).

[34] J. A. Buck, "Fundamentals of Optical Fibers," *John Wiley and Sons Inc.*, USA, 2nd Edition, 2004.

[35] K. Kaneshima, Y. Namihira, N. Zou, H. Higa, and Y. Nagata, "Numerical investigation of octagonal photonic crystal fibers with strong confinement field," *IEICE Transactions on Electronics*, vol. E89-C, no. 6, pp. 830-837, 2006.

[36] Y. Hibino and H. Hanafusa, "Formation mechanism of drawing induced peroxy radicals in pure silica optical fibers," *J. Appl. Phys.* Vol. **62**, pp. 1433, 1987.

[37] D. Ferrarini, L. Vincetti, M. Zoboli, A. Cucinotta, and S. Selleri, "Leakage properties of photonic crystal fibers," *Optics Express*, vol. 10, no. 23, pp.1314-1319, 2002.

[38] G. P. Agrawal, "Nonlinear Fiber Optics," *Academic Press*, 2nd Edition, 1995.

[39] Jonathan C. Knight, "Photonic crystal fibres," *Nature international weekly journal of science*, vol. 424, pp. 847-851, Aug. 2003.

[41] S. Olyaee and A. A. Dehghani, "High resolution and wide dynamic range pressure sensor based on two-dimensional photonic crystal," *Photonic Sensors*, vol. 2, no. 1, pp. 92–96, 2012.

[42] B. J. Mangan, L. Farr, A. Langford, P. J. Roberts, D. P. Williams, F. Couny, M. Lawman, M. Mason, S. Coupland, R. Flea, H. Sabert, T. A. Birks, J. C. Knight, and P S.Russell, "Low loss (1.7 dB/km) hollow core photonic bandgap fiber," *in Proceedings of Optical Fiber Communication Conference and Exhibition, OFC, PDP24* (Los Angeles, California, USA, 2004).

[43] L. P. Shen, W. P. Hung, and S. S. Jian, "Design and optimization of photonic crystal fibers for broadband dispersion compensation," *IEEE Photonics Technology Letters*, vol. 15, no. 4, pp. 540-542, Apr. 2003.

[44] T. A. Birks, J. C. Knight, and P. St. J. Russell, "Endlessly single-mode photonic crystal fiber, " *Optics Letters* , vol. 22, no. 13, pp. 961-963, July 1997.

[45] M. M. Haque, M. S. Rahman, M. Samiul Habib, M. Selim Habib, and S. M. A. Razzak, "A new circular photonic crystal fiber for effective dispersion compensation over E to L wavelength bands," *Journal of Microwaves, Optoelectronics and Electromagnetic Applications*, vol. 12, no. 2, pp. 281-291, Dec. 2013.

[46] Md. Selim Habib, Md. Samiul Habib, and S.M.A. Razzak, "Study on dual concentriccore dispersion compensating photonic crystal fiber," *International J. of Eng. And Technol.*, vol. 1, no. 4, pp. 377-383, 2012.

[47] K. Nagayama, M. Kakui, M. Matsui, T. Saitoh, and Y. Chigusa, "Ultra-low-loss (0.1484 dB/km) pure silica core fibre and extension of transmission distance," *Electron. Lett.* Vol. 38, pp. 1168, 2002.

[48] K. Tsujikawa, K. Tajima, and J. Zhou, "Reduction in optical loss of conventional and photonic crystal fibers," *in Proceedings of Optical Fiber Communication Conference andExhibition, OFC, WI5* (Los Angeles, California, USA, 2004).

[49] L. Farr, J. C. Knight, B. J. Mangan, and P. J. Roberts, "Low loss photonic crystal fibre," *in Proceedings of 28th European conference on optical communication*, PD1.3 (Copenhagen, 2002).

[50] K. Tajima, J. Zhou, K. Nakajima, and K. Sato, "Ultra low loss and long length photonic crystal fiber," *in Proceedings of Optical Fiber Communication Conference and Exhibition, OFC, Post Deadline* (Anaheim, CA, 2003).

[51] P.J.Bennett, T. M. Monro, and D. J. Richardson, "Toward practical holy fiber technology: fabrication, splicing, lvodelling, and characterization," *Opt. Lett.* Vol. **24**, pp. 1203,1999.

[52] A. A. Rifat, G.A. Mahdiraji, Y.M. Sua, Y.G. Shee, R. Ahmed, D.M. Chow, and F.R.M Adikan,"Surface plasmon resonance photonic crystal fiber biosensor: A practical sensing approach," *IEEE Photonics Tech. Lett.* Vol. 27, no. 15, 2015.

[53] M. R. Hasan , S. Akter, A.A. Rifat, S. Rana, and S. Ali, "A Highly Sensitive Gold-Coated Photonic Crystal Fiber Biosensor Based on Surface Plasmon Resonance," *Photonics,* vol. 4, no. 18, 2017.

[54] Brian H. Dennis, Weiya Jin, George S. Dulikravich, Jovo Jaric, "Application of the Finite Element Method to Inverse Problems in Solid Mechanics," *International Journal of Structural Changes in Solids*, vol. 3, no. 2, pp. 11-21, Jun. 2011.

[55] Fernando L. Teixeira, "Time-Domain Finite-Difference and Finite-Element Methods for Maxwell Equations in Complex Media," *IEEE TRANSACTIONS ON ANTENNAS AND PROPAGATION*, vol. 56, no. 8, pp. 2150-2166, Aug. 2008.

[56] S. Guo, F. Wu, S. Albin, H. Tai, and R. Rogowski, "Loss and dispersion analysis of Microstructured fibers by finite-difference method," *Optics Express,* vol. 12, pp.341-3352,2004.

[57] K. Saitohand, M.Koshiba, "Full-vectorial finite element beam propagation method with perfectly matched layers for an isotropic optical waveguides," *Journal of light wave technology,* vol. 19, p. 405, 2001.

[58] M. S. Islam, C. M. B. Cordeiro, M. A. R. Franco, J. Sultana, A. L. S. Cruz, and D. Abbott, "Terahertz optical fibers [Invited]," *Opt Express,* vol. 28, no. 11, pp. 16089-16117, May 25 2020.

[59] M. S. Islam *et al.*, "A novel approach for spectroscopic chemical identification using photonic crystal fiber in the terahertz regime," *IEEE Sensors Journal,* vol. 18, no. 2, pp. 575-582, 2017.

[60] M. S. Islam *et al.*, "A modified hexagonal photonic crystal fiber for terahertz applications," *Optical Materials,* vol. 79, pp. 336-339, 2018

[61] J. Sultana, M. S. Islam, M. Islam, and D. Abbott, "High numerical aperture, highly birefringent novel photonic crystal fibre for medical imaging applications," *Electronics Letters,* vol. 54, no. 2, pp. 61-62, 2017.

.